



**LEVEL II**

MS-EES-TR-81-1

2

TECHNICAL REPORT

DEGRADATION OF THE PERFORMANCE OF COMMUNICATION SYSTEMS  
IN THE PRESENCE OF INTERFERENCE

by

Shaw-Yueh Lin  
R. M. Showers

DTIC  
SELECTED  
APR 13 1981  
S  
C

Contract N00140-79-C-6628

with

Naval Underwater Systems Center  
New London Laboratory  
New London, CT 06320

University of Pennsylvania  
The Moore School of Electrical Engineering  
Department of Electrical Engineering and Science  
Philadelphia, Pennsylvania 19104

January 1981

DISTRIBUTION STATEMENT A  
Approved for public release:  
Distribution Unlimited

81 2 17 130

AD A 097 635

FILE COPY

147  
MS-EES-TR-81-1  
2

TECHNICAL REPORT, 147-1484

DEGRADATION OF THE PERFORMANCE OF COMMUNICATION SYSTEMS  
IN THE PRESENCE OF INTERFERENCE

by

10  
Shaw-Yueh Lin  
R. M. Showers



16

Contract N00140-79-C-6628

with

Naval Underwater Systems Center  
New London Laboratory  
New London, CT 06320

University of Pennsylvania  
The Moore School of Electrical Engineering  
Department of Electrical Engineering and Science  
Philadelphia, Pennsylvania 19104

11/51

11  
January 1981

388468

**DISTRIBUTION STATEMENT A**  
Approved for public release;  
Distribution Unlimited

UNCLASSIFIED

SECURITY CLASSIFICATION OF THIS PAGE (When Data Entered)

REPORT DOCUMENTATION PAGE		READ INSTRUCTIONS BEFORE COMPLETING FORM
1. REPORT NUMBER MS-EES-TR-81-1	2. GOVT ACCESSION NO. <b>AD-A097 685</b>	3. RECIPIENT'S CATALOG NUMBER
4. TITLE (and Subtitle) DEGRADATION OF THE PERFORMANCE OF COMMUNICATION SYSTEMS IN THE PRESENCE OF INTERFERENCE	5. TYPE OF REPORT & PERIOD COVERED Technical Report 1979-80	
	6. PERFORMING ORG. REPORT NUMBER	
7. AUTHOR(s) Shaw-Yueh Lin and R. M. Showers	8. CONTRACT OR GRANT NUMBER(s) N00140-79-C-6628	
9. PERFORMING ORGANIZATION NAME AND ADDRESS The Moore School of Electrical Engineering University of Pennsylvania Philadelphia, Pa. 19104	10. PROGRAM ELEMENT, PROJECT, TASK AREA & WORK UNIT NUMBERS	
11. CONTROLLING OFFICE NAME AND ADDRESS Naval Regional Contracting Office Philadelphia, Newport Division Building No. 132T, Newport, RI 02840	12. REPORT DATE January 1981	
	13. NUMBER OF PAGES	
14. MONITORING AGENCY NAME & ADDRESS (if different from Controlling Office) Code 344 Naval Underwater Systems Center New London Laboratory New London, CT 06321	15. SECURITY CLASS. (of this report) Unclassified	
	15a. DECLASSIFICATION/DOWNGRADING SCHEDULE	
16. DISTRIBUTION STATEMENT (of this Report) This report was prepared for the Naval Underwater Systems Center under contract N00140-79-C-6628. The release of all reports shall be with the expressed written consent of Code 344, Naval Underwater Systems Center, New London, CT 06321.		
17. DISTRIBUTION STATEMENT (of the abstract entered in Block 20, if different from Report)		
18. SUPPLEMENTARY NOTES		
19. KEY WORDS (Continue on reverse side if necessary and identify by block number) noise interference analog systems digital systems signal-to-interference ratios		
20. ABSTRACT (Continue on reverse side if necessary and identify by block number) The relationship between measures of degradation (for digital systems: error probability; and for analog systems: articulation score) has been examined for the purpose of establishing quantitative criteria for satisfactory performance of various modulation systems in the presence of various types of interference. Two empirical relationships are proposed which, with adjustment of only two parameter values, provide good correspondence between signal-to-interference ratio and the performance measure for each case.		

DD FORM 1 JAN 73 1473

EDITION OF 1 NOV 65 IS OBSOLETE

Unclassified

SECURITY CLASSIFICATION OF THIS PAGE (When Data Entered)

## ABSTRACT

The relationship between measures of degradation (for digital systems: error probability; and for analog systems: articulation score) has been examined for the purpose of establishing quantitative criteria for satisfactory performance of various modulation systems in the presence of various types of interference. Two empirical relationships are proposed which, with adjustment of only two parameter values, provide good correspondence between signal-to-interference ratio and the performance measure for each case.

## CONTENTS

	<u>Page</u>
Abstract.....	iii
List of Figures.....	v
1.0 INTRODUCTION.....	1
1.1 Approach.....	1
2.0 TOLERABLE LEVELS OF INTERFERENCE.....	1
2.1 Tolerable Signal-to-Noise Ratio.....	2
2.1.1 Digital Systems.....	2
2.1.2 Analog Systems.....	4
2.2 Tolerable Signal-to-Interference Ratio.....	4
2.2.1 Digital Systems.....	4
2.2.2 Analog Systems.....	9
2.2.3 Radar and Sonar Systems.....	9
3.0 RELATING SIGNAL-TO-INTERFERENCE RATIO TO DEGRADATION.....	16
3.1 Analog Systems.....	16
3.1.1 Examples of Curve Fitting.....	18
3.2 Digital Systems.....	31
4.0 CONCLUSIONS.....	40
5.0 REFERENCES.....	41

LIST OF FIGURES

<u>Figure No.</u>		<u>Page</u>
1	Error probability for various digital systems.....	3
2	Performance-degradation curve for CPSK system with analog interference.....	5
3	Performance of CPSK and ASK systems with impulse interference for fixed S/N values (results based on Ref. 18).....	7
4	Noncoherent reception of FSK from Ref. 3. Effects of coding. Parameters (n,k)-n = total number of digits in code word; k = no. of information digits.....	8
5	Performance-degradation curve of an AM voice system using an envelope detector with digital and voice interference. Refer to Ref. 13 for further detail.....	10
6	Performance degradation curves.....	11
7	Interference level for a 1-V, 1 $\mu$ s trapezoidal pulse and 1-V unit step (0.1 $\mu$ s rise time).....	12
8	Normalized spectrum $S_t(f)$ , dB (calculated with computer) and its bounds $R_t(f)$ , dB for linear FM trapezoidal pulse with rise and fall times of 1 $\mu$ s and duration 102 $\mu$ s. Line $\alpha$ represents improved bounds (from [27]). $f_b = 1/2$ bandwidth.....	14
9	Comparison of the logarithmic detector with the square-law detector for a false-alarm probability of $10^{-10}$ , and for n = 10 and 100 (quoted from [3]).....	15
10	Cochannel interference analysis between spaceborne and terrestrial radars (from Ref. 39).....	17
11	The function $A_s = \frac{1}{1 + ke^{-x/x_0}}$ .....	19
12	Comparison of experimental and modeled degradation curves; Analog Case, Example 1.....	21
13	Comparison of experimental and modeled degradation curves: Analog case, Example 2.....	25
14	Comparison of experimental and modeled degradation curves: Analog case, Example 3.....	29

Continued

LIST OF FIGURES

<u>Figure No.</u>		<u>Page</u>
15	Error probability for various digital systems. Effects of CW interference.....	32
16	Comparison of modeled and theoretical error probability curves: Digital case, Example 2.....	36
17	The Function $P_e = \frac{1}{2} e^{-x^n/x_0}$ .....	38

TABLES

Table I	Comparison of approximation formula for articulation score ( $A_s$ ) with experimental curve (example 1).....	23
Table II	Comparison of approximation formula for articulation score ( $A_s$ ) with experimental curve (example 2).....	26
Table III	Comparison of approximation formula for articulation score with experimental curve (example 3).....	30
Table IV	Comparison of coherent PSK performance curve in Gaussian noise with approximated curve.....	35

## 1.0 INTRODUCTION

Methods of predicting mutual electromagnetic compatibility of various assemblies of electrical and electronic systems have been developed over the years. Because of the complexity of many of the electromagnetic interactions that occur, generally use is made of computer procedures based upon either measured or modeled equipment data. The models are, in some cases, very sophisticated.

One of the weakest capabilities of present techniques, however, is the assessment of the degradation to be expected when interference is evident on any particular device or system. For example, although it is possible to predict whether or not interference will appear on a radar receiver, it does not always result in serious degradation of operation because many radar operators can "read through" many types of interference. Furthermore, special circuits such as noise cancellers, noise suppressors, or blankers, which can be effective in reducing otherwise degrading effects, should be taken into account in the prediction procedure.

It is the purpose of this report to explore the various phenomena involved in degradation and then to determine procedures that can be used to provide quantitative estimates. It is clear that with a given signal source, a given type of interference, and a given application, some sort of empirical relationship can always be agreed upon. A measure of success for this undertaking will be the extent to which such empirical relations can be generalized so as to provide relatively simple procedures applicable to many, if not most, combinations of signal and interference.

### 1.1 Approach

In the first part of this report the discussion is concerned with a review of the literature covering the interaction of various types of signal and interference and the definition of possible measures of degradation. As shall be seen, in some combinations the measures are relatively straightforward. In others, however, the measures may be more complex. In the second part, empirical relations between signal-to-interference ratio and degradation measures are formulated and validated. A separate report, to be published in the future, will deal with the possibility of generalizing the relations and with semi-analytic methods of computing the degradation for various signal modulation and interference types.

## 2.0 TOLERABLE LEVELS OF INTERFERENCE

Requirements for reducing emission levels from radiators having a potential for producing output interference are usually established in terms of the "tolerable" ratio of input signal-to-interference level.\*

---

\* The term "Protection Ratio" in CCIR and some other literature is used to identify the "tolerable" S/I, as used in this report.

This ratio is, in turn, a function of several factors, including the type of information transmitted, modulation used, receiver design (particularly detectors and input circuits), bandwidth used, and the nature of the extraneous input encountered.

As a criterion in performance analysis, the threshold input signal-to-interference (S/I) ratio can be defined as the lowest value for which the output of the final receiver detector provides satisfactory system performance. Determination of the critical point is a somewhat subjective matter, especially in systems with a "soft" characteristic, such as in AM-envelope and square-law detection systems. A sharp threshold characteristic may appear in FM systems. The softness of the characteristic is closely related to the demodulation process used (Ref. 1).

## 2.1 Tolerable Signal-to-Noise Ratio

Since Gaussian noise is the reference to which other forms of interference are compared, its effects are described first.

### 2.1.1 Digital Systems

In digital systems, it is relatively easy to identify a readily acceptable performance criterion, namely probability of error  $P_e$ , provided errors are distributed somewhat randomly. (A different criterion would be required for errors that occur in bursts.)

Modulation techniques commonly used for digital transmission encompass amplitude-shift keying (ASK), including the long used on-off keying (OOK), phase-shift keying (PSK), and frequency-shift keying (FSK). Further classification splits these techniques into coherent or non-coherent and synchronous or asynchronous categories (Refs. 2-4).

Figure 1 shows  $P_e$  plotted vs digital signal-to-noise (S/N) ratio at the input to the detector for several systems (Refs. 3,4). Continuous-phase, frequency-shift keying (CPFSK), either coherent with a three-bit decision scheme or noncoherent with a five-bit decision scheme, has a slight advantage over a CPSK system for high S/N regions (Refs. 5,6). It also has been proven (Ref. 7) that performance identical to that of coherent phase-shift keying (CPSK) on a linear, infinite-bandwidth, white Gaussian noise ideal reference channel can be achieved either as a special case of CPFSK with a deviation ratio 0.5 (Ref. 8), or as one of a class of quadrature modulation waveforms (Ref. 9), or as a staggered quaternary PSK system (Ref. 9), which is also one of a class of quadrature modulation systems with rectangular modulation waveform (Ref. 9). Many other newly-developed systems, such as amplitude-phase keying (APK), phase-comparison sinusoidal frequency-shift keying (PCSFSK), quadrature amplitude modulation (QAM), etc., achieve similar performance improvements to a greater or lesser degree (Refs. 10, 11).

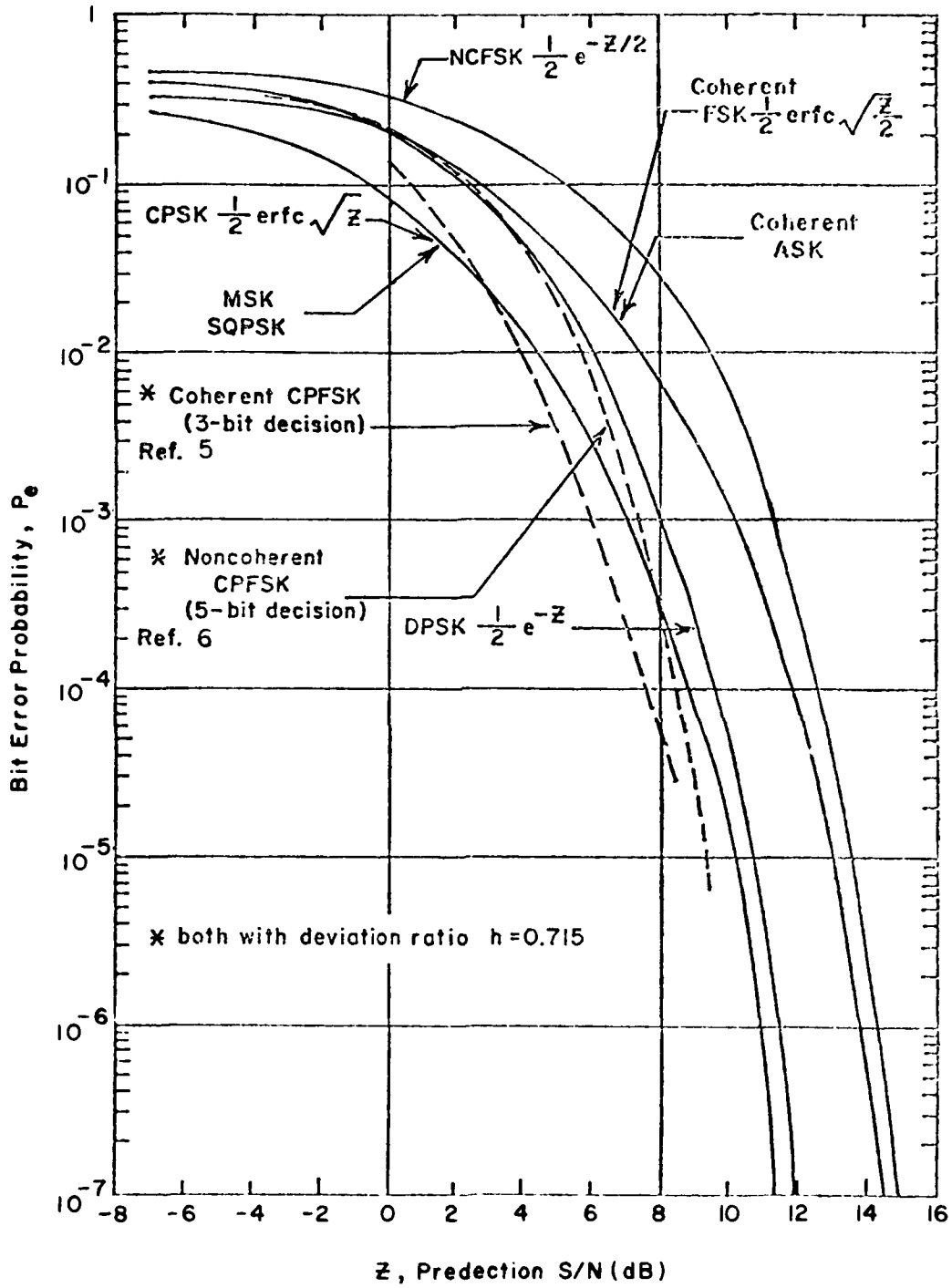


Figure 1 Error Probability for Various Digital Systems

### 2.1.2 Analog Systems

In an analog system, it is best to consider performance evaluation as a two-step process because, for voice or video, a subjective criterion of performance must be imposed. One determines, for various modulation systems, S/I at the detector output as a function of S/I at the input, and then relates the output S/I to the subjective performance criterion.

In a voice system, articulation score (AS), or the articulation index (AI), may be used. In other analog systems, mean-square error may be a suitable parameter indicating a fidelity criterion. The articulation score is the percentage of words transmitted that are received correctly (Ref. 12). The articulation index (AI) is obtained by a weighting of values of signal and noise over segments of the audio-frequency band (Ref. 13). The word articulation score in the presence of continuous noise output is about 50% for an S/N of 0 dB. For an articulation score of 85% using a typical word list, an S/N of 10 dB is required. Tolerable S/N values for several practical analog systems are found in (Ref. 13).

### 2.2 Tolerable Signal-to-Interference Ratio

In contrast with Gaussian noise, interference inputs can have various non-Gaussian forms, of which sine waves and impulses are extreme examples. Because of the wide variety of such waveforms, it is not possible to cover all cases here. However, some examples will serve to indicate the effect that can be observed and, through classification of interference waveforms, it should be possible, in most instances, to obtain reasonable estimates of the degradation to be observed on particular desired signals.

#### 2.2.1 Digital Systems

a) Interfering Signals: Basic types of interfering signals are used for evaluating co-channel and adjacent-channel interference. Analysis procedures for various digital systems may be found in Refs. 14 to 16.

One of the noteworthy effects of a pure CW signal on digital systems is the appearance of a sharp threshold. The sharp-threshold effect (Ref. 14) is somewhat smoothed by the presence of modulation of the interference waveform and by internal noise (Ref. 17). Figure 2 shows the case when an analog undesired signal is introduced into a CPSK system in which S/N values of 6.65 and 8.81 dB exist. If internal (Gaussian) noise were absent, the threshold S/I would be 0 dB. An S/I of 20 dB is required with an S/N of 8.81 dB to assure an error probability of less than  $10^{-4}$ .

b) Impulsive Interference: The performance of digital systems under the influence of apparently Gaussian noise is frequently not in close agreement with theory. The discrepancy can be attributed to the fact that often the main source of noise is, in fact, non-Gaussian. A study of the combined effects of Gaussian and impulse noise (interference) (Ref. 18) shows that, for the low S/N region, Gaussian noise generally dominates. For the high S/N range, impulsive noise serves as the limiting factor.

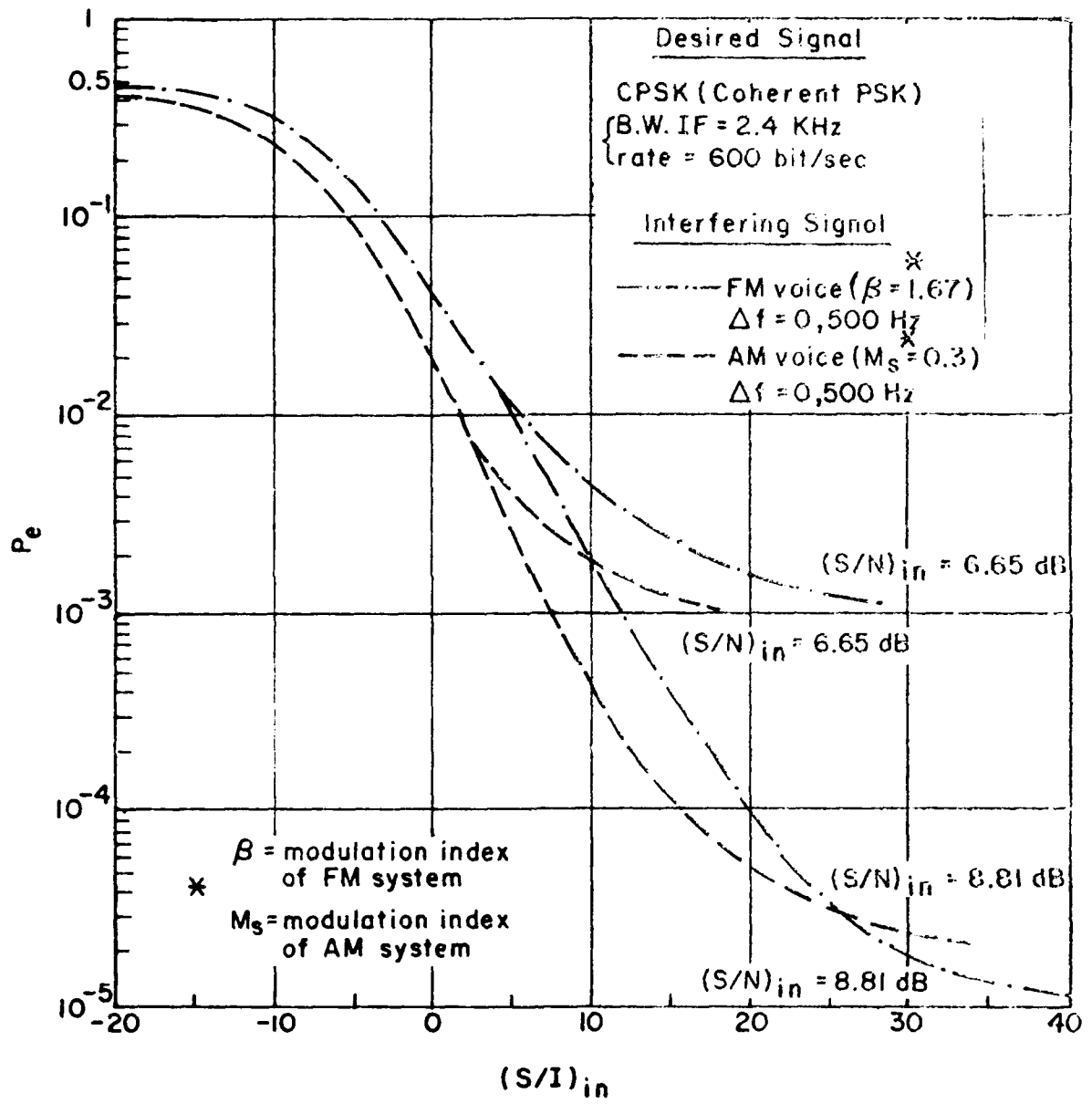


Figure 2 Performance-Degradation Curve for CPSK System With Analog Interference

Sources of impulsive noise are generally categorized into man-made and natural disturbances. Due to the non-ergodic property of impulsive noise, a complete statistical description is generally difficult. A historic survey of the development of the statistics of impulse noise can be found in Ref. 19. Recently, Middleton has proposed a canonical model for both narrow-band and wideband impulsive sources, which provides more detailed mathematical formulation and agrees with experimental results quite accurately in many cases (Refs. 20,21).

Figure 3 shows impulsive-interference effects on CPSK and ASK systems for given levels of S/N (Ref. 18). It should be noted that performance as a function of extraneous-input level can be sharply influenced by the S/N value.

Various techniques have been introduced to suppress the effect of impulse noise to improve the system performance. Examples are noise limiters and the smear-desmear technique developed some time ago, and the use of nonlinear processing (Refs. 22,23).

c) Effects of Coding: Most of the analyses of the improvement in transmission quality by using codes have been made for an additive Gaussian-noise environment. Several important results, which prove to hold even when the extraneous input is not Gaussian, are:

1. Coding may provide improvement under some conditions of extraneous input and degradation under others. A typical example of MFSK employing two group codes of different lengths is shown in Fig. 4. Favorable performance occurs generally only for high S/N (Ref. 3). In the low S/N region, performance may be poorer than for the uncoded system.

2. In performance evaluation, word error probability  $P_w$  and bit error probability  $P_e$  must be carefully distinguished. It is shown (Ref. 24) that, for any group error-correcting code,  $P_w$  is never exceeded by its corresponding  $P_e$  of information bit (for Gaussian noise and pulse interference).

3. The performance of an error-correcting code is generally improved as the code length or encoded bit-stream size increases (Ref.4).

The important question is how various coding schemes perform when the system is subjected to particular types of undesired signals, such as pulse or CW (Refs. 24-26). Pulsed interference of relatively low duty cycle may produce bursts of errors (Ref. 25). Proper choice of coding schemes, by taking undesired signals into consideration, can achieve an encouraging improvement in system performance.

Generally speaking, since the coding gain for schemes of moderate complexity applies to specific types of undesired input, unexpected types can produce degradation not at all ameliorated by the coding scheme adopted.

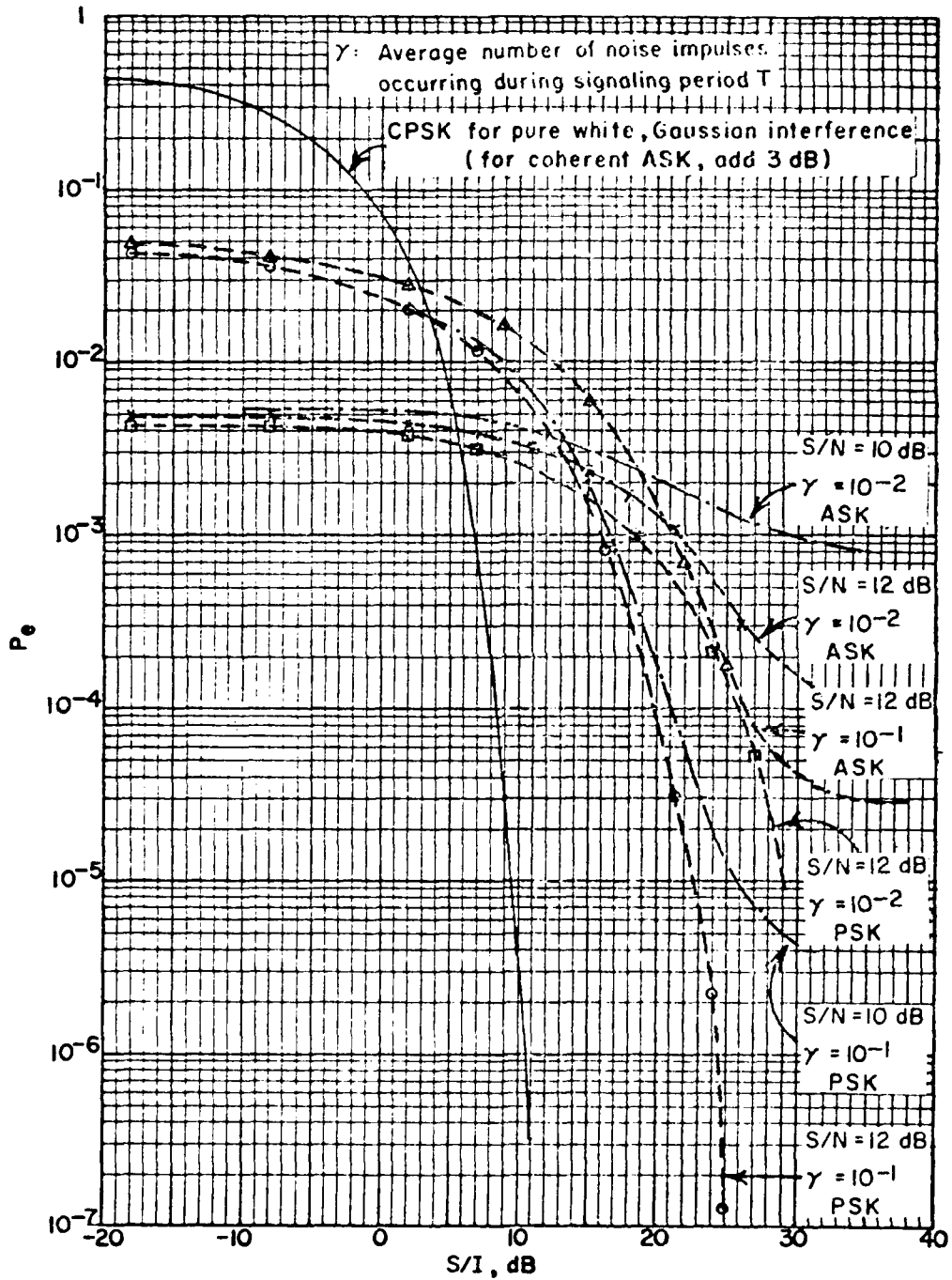


Figure 3 Performance of CPSK and ASK Systems With Impulsive Interference for Fixed S/N Values (results based on Ref. 18)

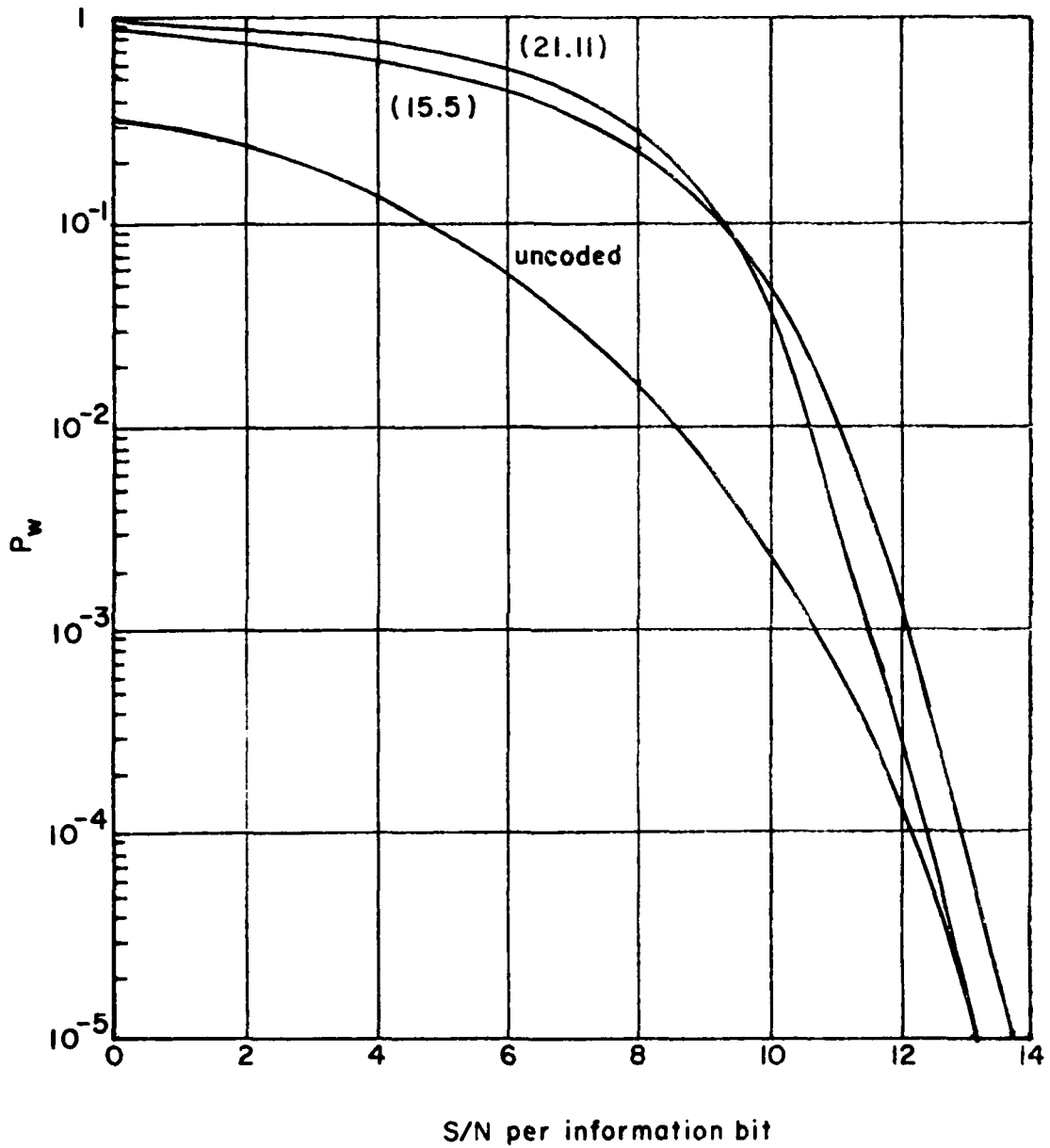


Figure 4 Noncoherent Reception of FSK From Ref. 3. Effects of Coding. Parameters  $(n, k)$  -  $n$  = Total Number of Digits in Code Word;  $k$  = No. of Information Digits

### 2.2.2 Analog Systems

Due to the inherently "subjective" performance criteria used and the various forms of undesired input, care must be taken to insure that meaningful results are achieved. For example, the automated Articulation Index method has been shown to provide rather constant relationships with respect to the Articulation Score for white noise (Ref. 13). It apparently holds fairly well for other relatively continuous sources, but is not readily relatable for discontinuous-type sources, typical of pulsed signals, ignition noise, etc. An extensive set of performance-degradation data, including threshold tables and degradation curves, for various digital and analog systems is available (Ref. 13).

Figure 5 gives an example of the performance degradation of an AM signal by an FSK digital signal or by an FM voice signal. S/I ratios are based upon average values of extraneous voice signals and peak values of extraneous digital signals. The effects of internal noise  $N$  can be seen as similar to that of detuning. One interesting point should be noted:

ON-tune undesired digital or analog sources degrade less seriously than somewhat OFF-tune ( $\Delta f = 500$  Hz) sources, largely because of the beat note produced when the interferer is slightly off-tune. The effect varies for different S/N levels and digital bit rates.

For the cases shown in Fig. 5, it is concluded that an S/I level of 10 dB is a reasonable value (except for high-quality service) for operation of an AM voice system either in the presence of analog or digital interference, since the AS will be well above the 50% value.

Shown in Fig. 6 are  $A_s$  vs (S/I) for several kinds of interference. It is not surprising to find out that white noise interference is the most effective in degrading speech, while highly redundant interference such as pure tone and pulse interference are relatively ineffective in degradation of speech. Furthermore, parameters such as the transmission rate of pulse signal and the frequencies of tones influence the performance significantly.

### 2.2.3 Radar and Sonar Systems

Due to their distinctive operating characteristics, radar and sonar systems are discussed separately from the more standard types of "communication" systems.

The spectra shown on Fig. 7 are typical of some radars since they also apply to a single-pulse-modulated carrier, if the zero-frequency point on Fig. 7 is considered to correspond with the frequency of the carrier. A reflection about the ordinate of the spectral curve on Fig. 7 applies to frequencies below the carrier. In use, when a circuit has a response over a (narrow) effective impulse bandwidth  $\Delta f$ , the peak voltage of the transient in the circuit is obtained by multiplying the spectrum amplitude on Fig. 7 by the effective impulse bandwidth.

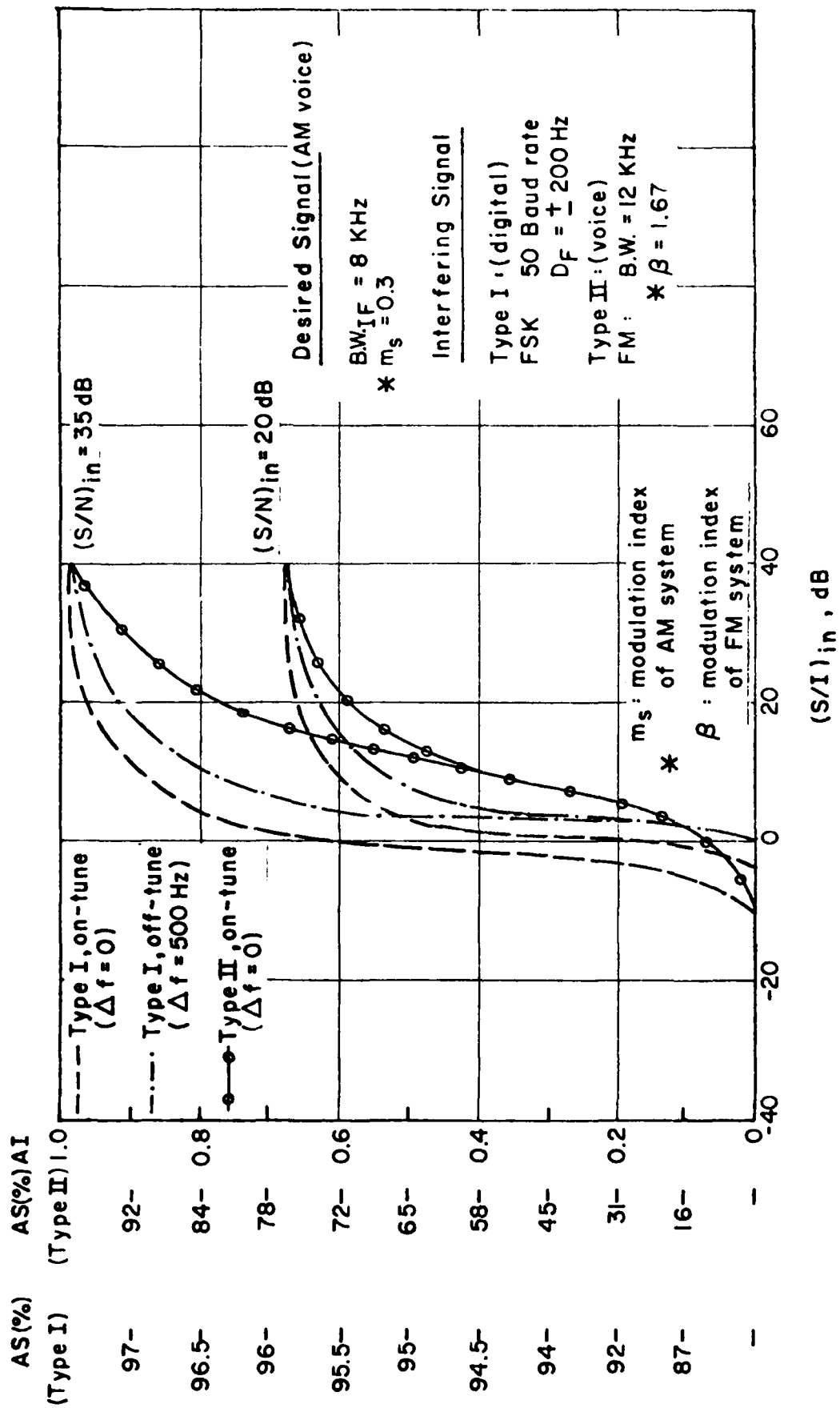


Figure 5 Performance-Degradation Curve of an AM Voice System Using an Envelope Detector With Digital and Voice Interference. Refer to Ref.13 for Further Detail.

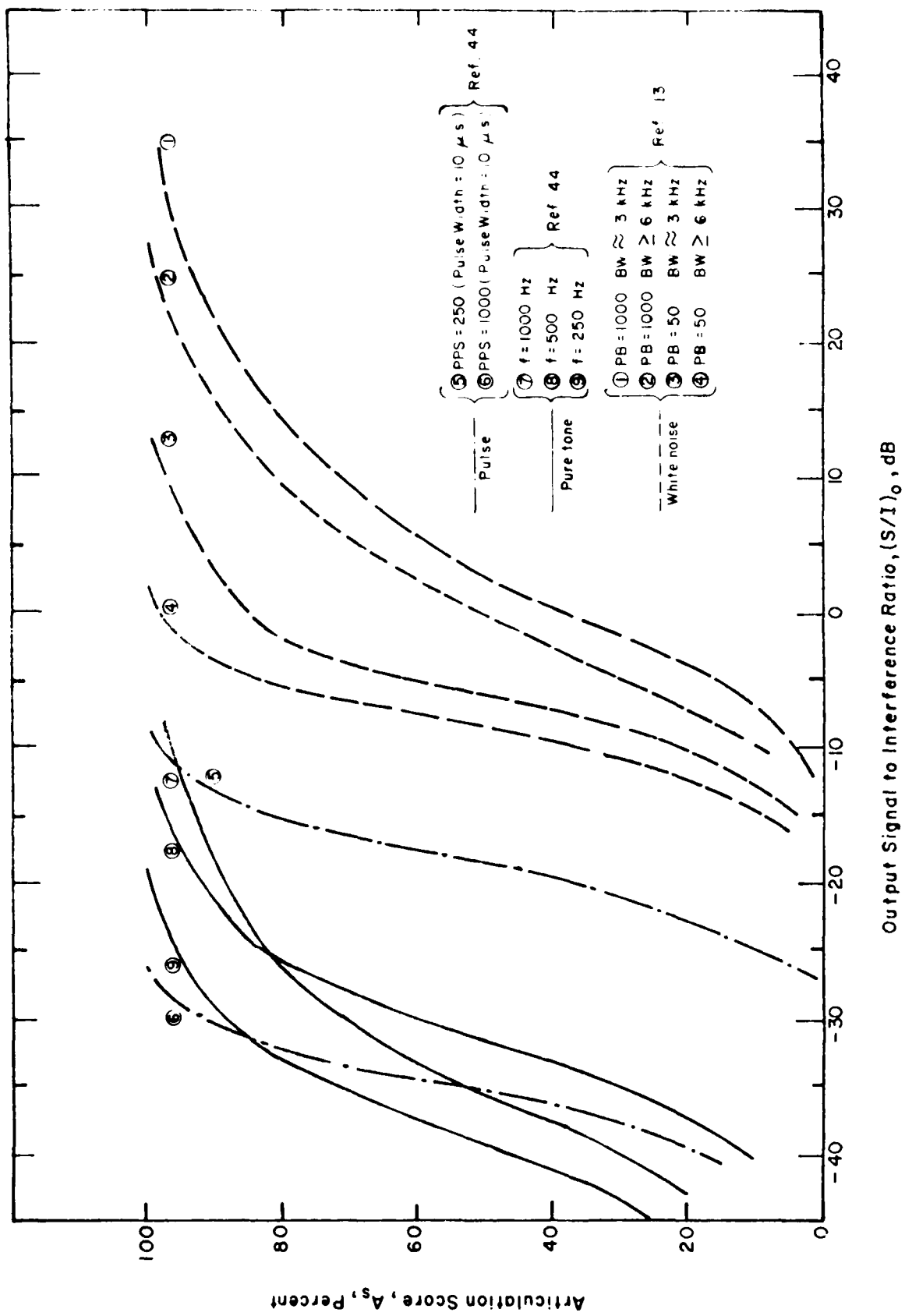
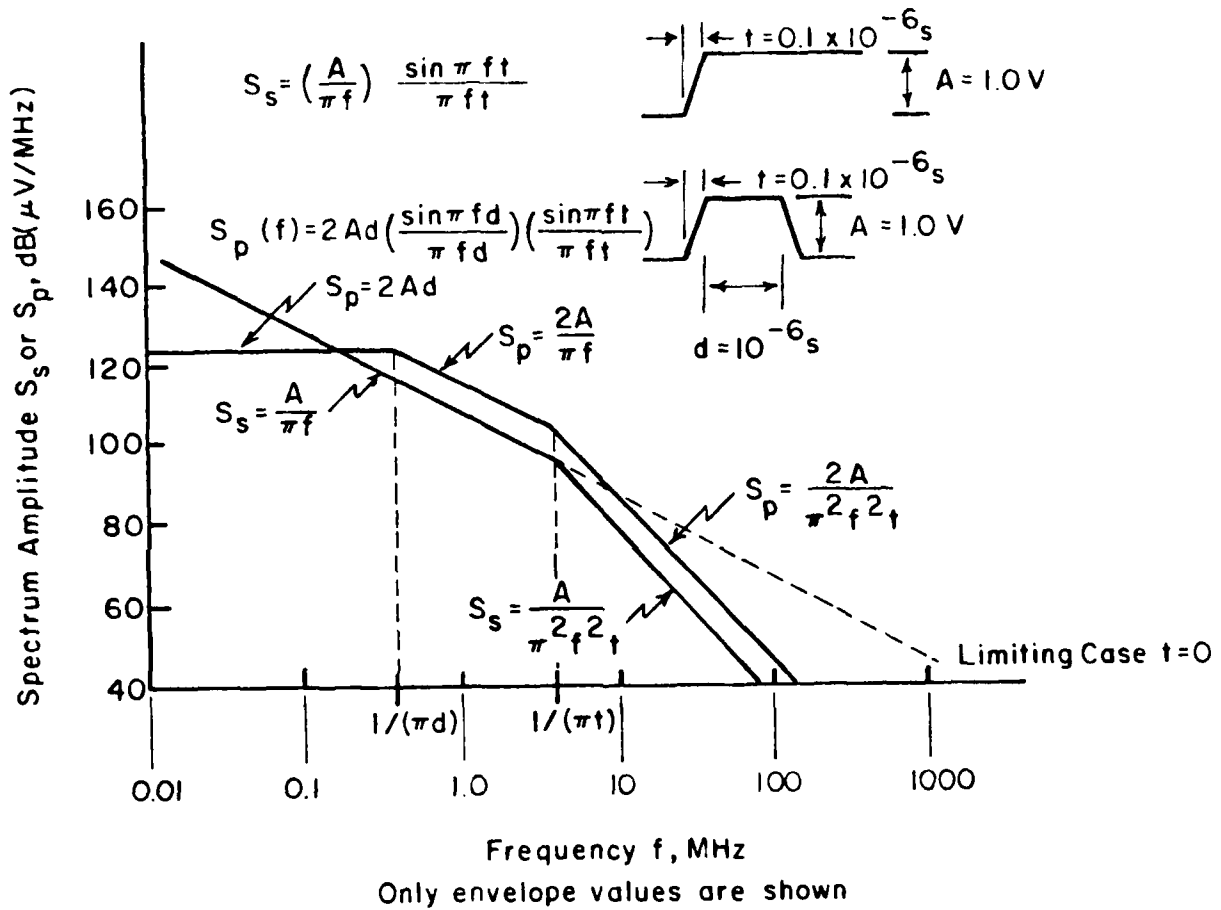


Figure 6 Performance Degradation Curves



Refer to formulas for other shapes (different  $t$ ,  $A$ , or  $d$ )

Figure 7 Interference Level for a 1-V, 1  $\mu$ s Trapezoidal Pulse and 1-V Unit Step (0.1  $\mu$ s Rise Time)

Although the spectrum bounds of Fig. 7 apply to a single-pulse AM-modulated carrier of fixed frequency, they no longer apply to an FM-modulated pulse, commonly used in CHIRP radar. For linear frequency-modulated pulses, bounds also exist; they depend upon the shape of the pulse. Figure 8 illustrates the case of a linear FM, symmetrical, trapezoidal pulse with rise and fall times of 1  $\mu$ s and duration 102  $\mu$ s. This as well as rectangular, unsymmetrical, trapezoidal and Hamming-weighted cases may be found in Ref. 27.

The basic operation performed by either a radar or sonar system is "detection," i.e., determining if a certain type of "target" is present. Performance in the presence of Gaussian noise is usually measured in terms of well-formulated statistical signal-detection theory. Some general discussion, including basic estimation theory commonly used, may be found in Refs. 2, 28.

Various optimum detectors have been developed (Ref. 29). Figure 9 shows typical performance curves for logarithmic and square-law detectors. It shows the probability of detection (PD) vs received S/N ratio, with constant probability of false alarm (Ref. 30) as a parameter. In systems where post-detection integration (Ref. 30) is used, the number  $n$  of pulses integrated can influence the result significantly.

Other techniques have been developed to select certain types of "targets". An example is the use of moving-target indicators (MTI). Though effective in stationary clutter (see below) and other respects (Ref. 31), S/N degradation occurs under certain conditions (Refs. 32,33).

Interference encountered in these systems may be classified as either: (a) clutter (or reverberation in sonar), or (b) intersystem (mutual). Clutter is a special type of interference not usually encountered in communication systems, except for multipath effects (not an effect between different systems). It originates either from back-scattering of outgoing signals from multiple targets (self-clutter) or from various environmental effects. It may cause serious degradation in detection probability, reduce resolution, overload low-level signal processing, and induce other deleterious effects. For a further understanding of its statistics and harmful effects, see Refs. 34 to 36.

Much attention has been given to this type of interference by both radar and sonar designers. Due to its non-ergodic characteristics, optimum general approaches to combat it are not possible. However, particular methods of both signal and circuit designs may successfully reduce it. For detailed discussions in this field Refs. 35 to 37 should be useful. It is to be noted that passive radar or sonar systems (Ref.38) are free of this type of interference.

Due to the expanded use of radars, not only for military, but also for civilian applications, mutual-interference problems have become more important. A recent work by Nicholas (Ref. 39) discusses cochannel

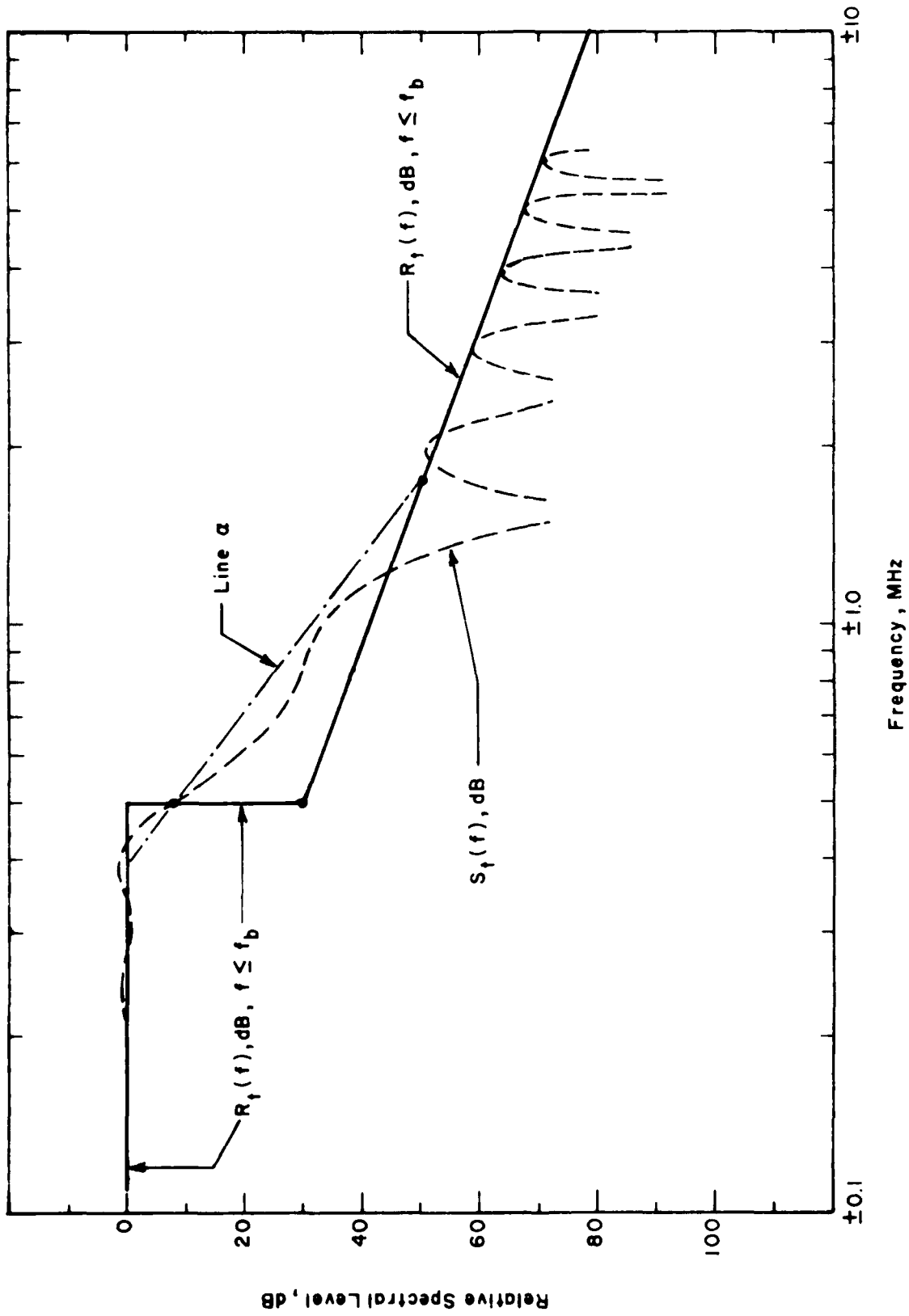


Figure 8 Normalized Spectrum  $S_t(f)$ , dB (calculated with computer) and its Bounds  $R_t(f)$ , dB for Linear FM Trapezoidal Pulse With Rise and Fall Times of  $1 \mu\text{s}$  and Duration  $102 \mu\text{s}$  Line  $\alpha$  Represents Improved Bounds (from [27]).  $f_b = \frac{1}{2}$  Bandwidth

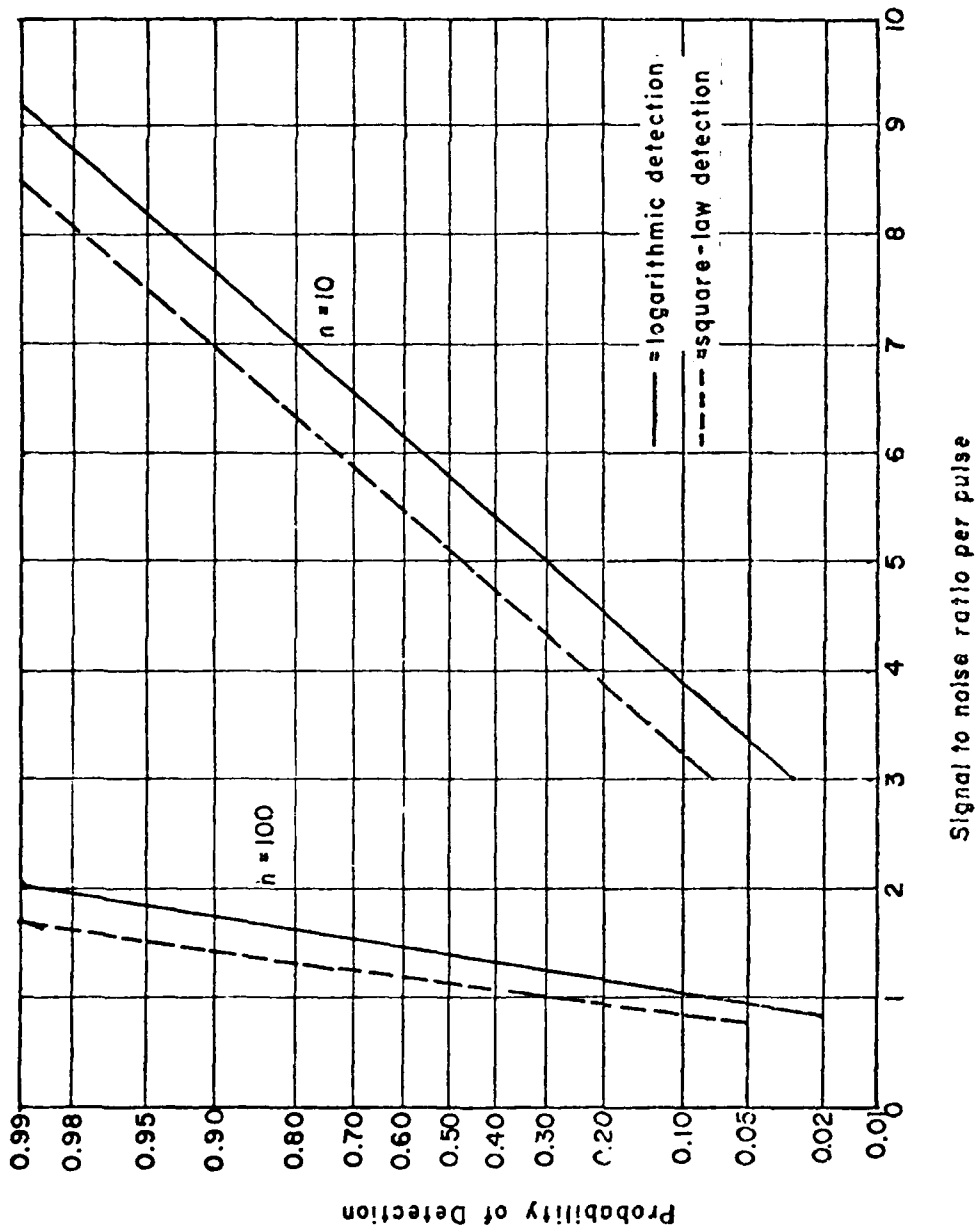


Figure 9 Comparison of the Logarithmic Detector With the Square-law Detector for a False-alarm Probability of  $10^{-10}$ , and for  $n=10$  and  $100$  (Quoted From [3])

interference between spaceborne and terrestrial radars (see Fig.10). The ordinate T is a measure of performance, i.e., percent of time spaceborne radars produce power that exceeds the minimum discernible signal (MDS) of the terrestrial radar. The abscissa is the number of spaceborne radars. The parameter on each curve is the ratio of the spaceborne radiated power to the MDS power of the terrestrial radar.

The effects of radar interference on search-radar operator performance are discussed in Refs. 40 and 41. Simulation results indicate that in no case was operator performance significantly affected by a displayed pulse count of 100 or less (due to one or more search radars). Consequently, this value may be considered at least an interim threshold or limit for permissible interference due to interactions among search radars.

Various techniques have been proposed to prevent the harmful effects of mutual interference, or at least to suppress them to a tolerable degree. Among them are blanking, pulse width and pulse repetition frequency discrimination, Lamb noise-silencing circuits, side-lobe cancellations, etc. Details of these techniques are found in Refs. 30, 42, and 43.

### 3.0 RELATING SIGNAL-TO-INTERFERENCE RATIO TO DEGRADATION

The preceding discussion provides the basis for relating the signal-to-interference ratio to performance measures such as articulation score and bit error rate. In the following, simple functional expressions relating these quantities are postulated. Later, examples are given which demonstrate the validity of the expressions. The expression is used in opposite ways in evaluating digital and analog systems. In the digital case the expression gives the "negative" quality of bit error rate, whereas in the analog case the expression is inverted to give the "positive" quality of articulation index. We discuss the analog case first.

#### 3.1 Analog Systems

The proposed expression is:

$$A_s = \frac{1}{1 + k e^{-x/x_0}} \quad (1)$$

where

$A_s$  is the articulation score

$k$  and  $x_0$  are constants, selected for particular types of signal and interference combinations

$x$  is the appropriate signal-to-interference power ratio, which is expressed in dB.

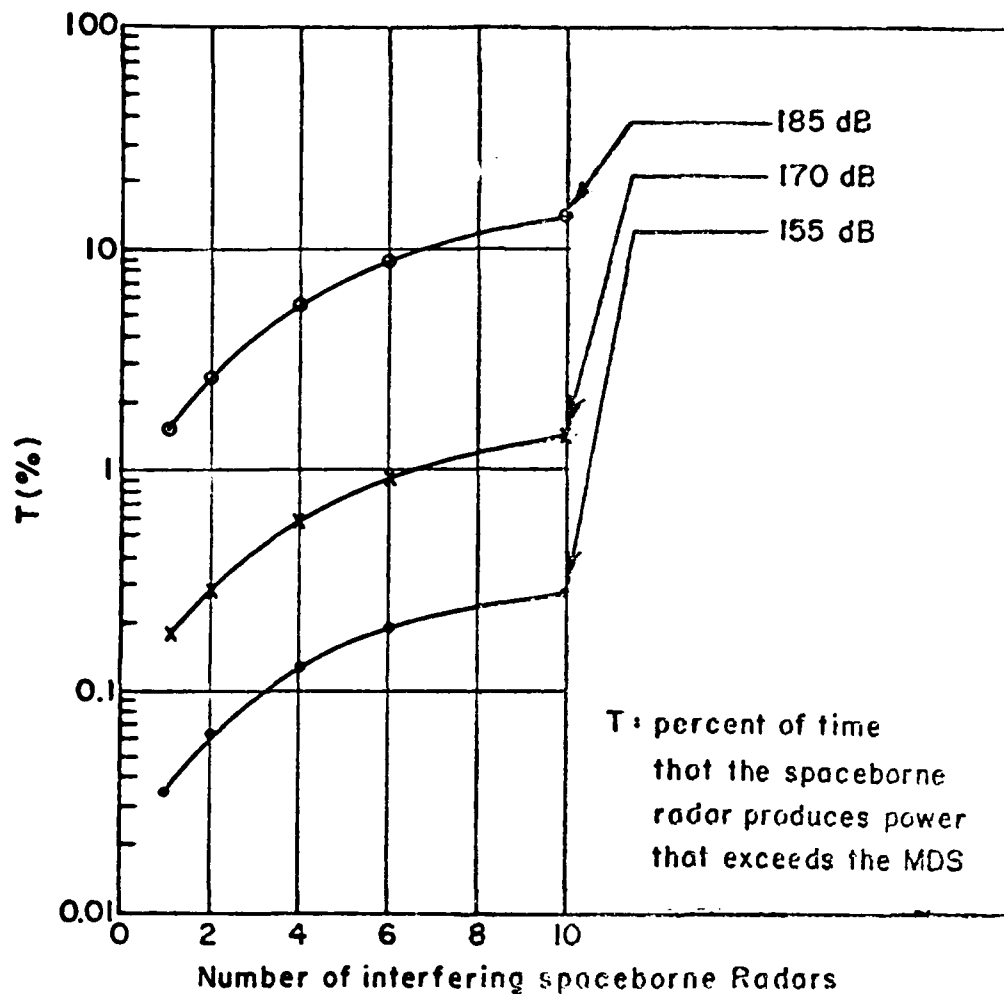


Figure 10 Cochannel Interference Analysis Between Spaceborne and Terrestrial Radars (From Ref. 39)

Equation 1 approaches zero when  $x$  approaches  $-\infty$ , and approaches 1 when  $x$  is close to  $\infty$ , therefore satisfying the extreme S/I conditions.

It can be seen that  $x_0$  is the dominant factor in the shape of the curve in the vicinity of  $x = x_0$ .

Furthermore, suppose that we have two curves of the same shape, except for a relative shift of  $(S/I) = x_s$ . Then, from (1)

$$\begin{aligned}
 A_s &= \frac{1}{1 + k' e^{-(x-x_s)/x_0}} \\
 &= \frac{1}{1 + \left(k' e^{x_s/x_0}\right) e^{-x/x_0}} \\
 &= \frac{1}{1 + k e^{-x/x_0}} \quad (2)
 \end{aligned}$$

where  $k = k' e^{x_s/x_0}$

Without loss of generality, we can let  $k' = 1$ , thus

$$k = e^{x_s/x_0} \quad (3)$$

For any given experimental curve the values of  $k$  and  $x$  can be determined by matching 2 points of the curve or graphically as follows. Figure 11 is a plot of Eq. 1 for  $k = 1$  and various values of  $x_0$ . One first finds the curve on Fig. 11 which best matches the shape of the experimental curve regardless of any relative horizontal displacement along the S/I axis. This establishes the value of  $x_0$ . Next, the horizontal displacement  $x$  of the theoretical and experimental curves for the point of the ordinate = 0.5 is observed and designated  $x_s$ . The value of  $k$  is then obtained from (3).

### 3.1.1 Examples of Curve Fitting

Using (1), one selects two known points of an experimental curve  $(A_{s1}, x_1)$  and  $(A_{s2}, x_2)$  and one can determine  $(k, x_0)$  by the relations

$$x_0 = \frac{(x_2 - x_1)}{\ln \left[ \frac{(1 - A_{s1}) A_{s2}}{(1 - A_{s2}) A_{s1}} \right]} \quad (4)$$

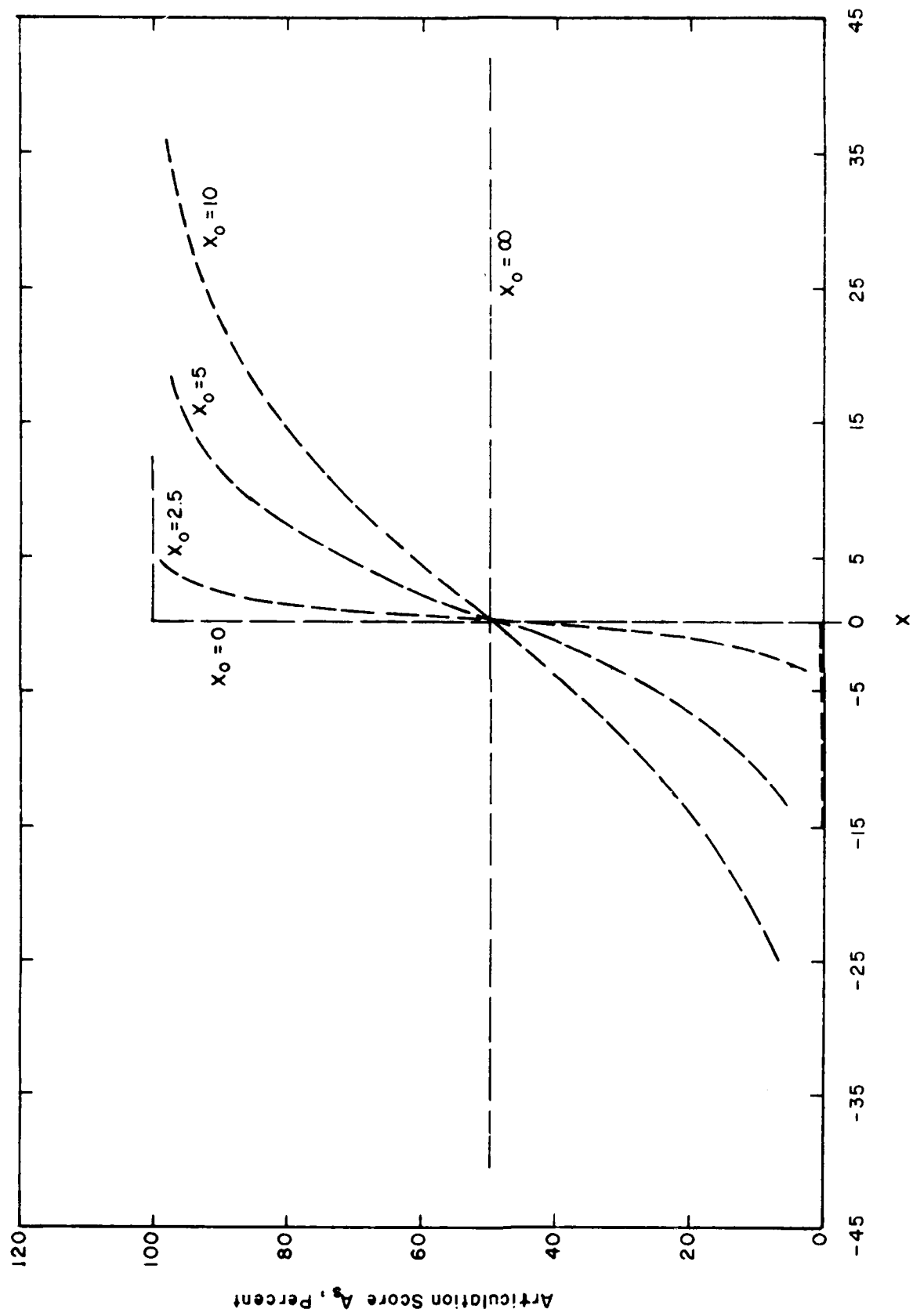


Figure 11 The Function  $A_s = \frac{1}{1 + ke^{-X/X_0}}$

$$k = \begin{pmatrix} 1-A_{s1} \\ A_{s1} \end{pmatrix} e^{x_1/x_0} \quad i = 1,2 \quad (5)$$

The validity of the values  $(k, x_0)$  obtained from (4) and (5) for other values of  $x$  can be determined. Figure 6 shows a variety of  $A_s$  vs  $(S/I)_0$  curves that have been discussed in previous sections of this report.

#### Example 1

The curve marked ⑤ on Fig. 6 is for a 10  $\mu$ s, 250 cps pulse interference. The  $A_s$  vs  $(S/I)_0$  curve is discussed on pp. 3-12 of Ref. 44 (plotted as the solid line in Fig. 12).

First, try fitting the experimental curve at somewhat extreme values of  $A_s$ , for example,  $A_s = 0.8$  and  $0.2$ . Thus, one has corresponding values of  $S/I = -6.25$  dB and  $-12.5$  dB, respectively, or

$$(A_{s1}, x_1) = (0.8, -6.25 \text{ dB})$$

$$(A_{s2}, x_2) = (0.2, -12.5 \text{ dB})$$

Thus, using Eqs. 4 and 5

$$A_s = 0.2 \quad S/I = -12.5 \text{ dB}$$

$$A_s = 0.8 \quad S/I = -6.25 \text{ dB}$$

$$z_0 = \frac{(x_2 - x_1)}{\ln \left\{ \frac{(1-A_{s1})A_{s2}}{A_{s1}(1-A_{s2})} \right\}} = \frac{6.25}{\ln \left( \frac{0.2}{0.8} \right)} = 2.254$$

$$k = \frac{1-0.2}{0.2} e^{-12.5/2.254} = 0.0156$$

$$A'_s = \frac{1}{1 + 0.0156 e^{-x/2.254}}$$

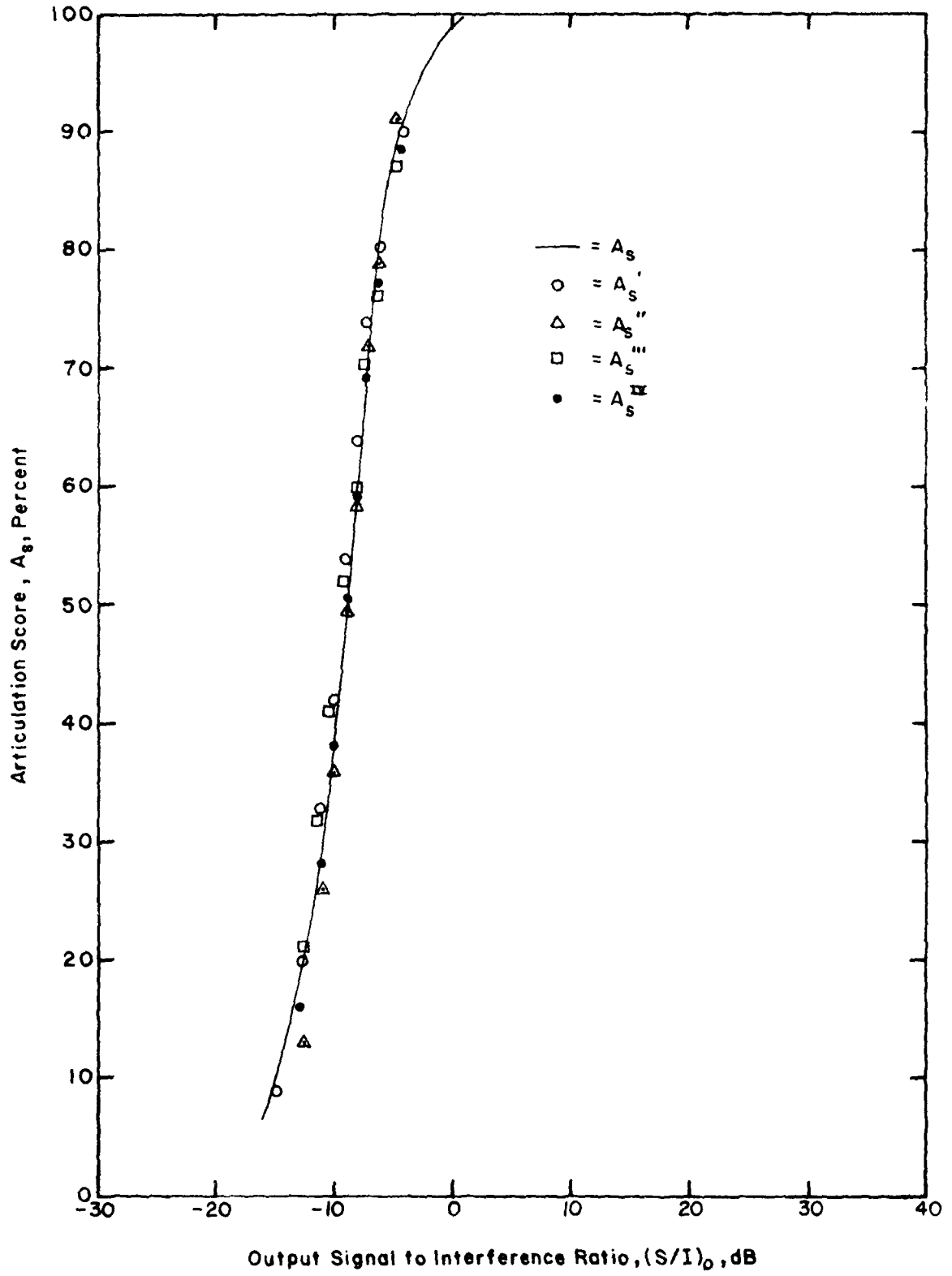


Figure 12 Comparison of Experimental and Modeled Degradation Curves: Analog Case, Example I

The results obtained are shown in Table I in the third and fourth columns. Note that, for an articulation score of 0.5, the error is 5%. While this is small, it is a region that might be considered for some applications to be critical. Since usually the performance is unsatisfactory for articulation scores of less than 0.5, one might prefer good accuracy at this value and higher. Hence, try the following:

$$(A_{s1}, x_1) = (0.6 - 8.10)$$

$$(A_{s2}, x_2) = (0.5 - 8.90)$$

With formulas 4 and 5

$$x_0'' = 1.973$$

$$k'' = 0.011$$

The 6th column of Table I shows the error in the articulation score  $A_s''$  as compared with the experimental (true) value.  $A_s''$  is shown in Fig. 12 as a dashed curve. The approximation is not very good in the low (S/I) region. For the same case, we choose another two points

$$(A_{s1}, x_1) = (0.7, -7)$$

$$(A_{s2}, x_2) = (0.6, -8.1)$$

Then

$$x_0''' = 2.48$$

$$k''' = 0.025$$

$(A_s''' - A_s)$  is tabulated in the 8th column of Table I. This time, the approximation in the low (S/I) region is improved compared with  $A_s''$ . But in the high S/I region, a slightly pessimistic prediction is seen.  $A_s'''$  is also plotted in Fig. 12 for comparison.

It is natural, then, to seek an intermediate value of  $(k, x_0)$  from the above two results.

TABLE I  
 COMPARISON OF APPROXIMATION FORMULA FOR ARTICULATION SCORE ( $A_S$ ) WITH EXPERIMENTAL CURVE (EXAMPLE I)

$A_S$	$x$ (dB)	Points Matched										$x_0^{IV} = (x_0^{II} + x_0^{III})/2, k^{IV} = (k^{II} + k^{III})/2$
		$A_S = 0.8, 0.2$		$A_S = 0.6, 0.5$		$A_S = 0.7, 0.6$		$A_S^{III} - A_S^{(.)}$		$A_S^{IV} - A_S^{(.)}$		
		$A_S'$	$(A_S' - A_S)^{(\%)}$	$A_S''$	$A_S'' - A_S^{(\%)}$	$A_S'''$	$A_S''' - A_S^{(.)}$	$A_S^{IV}$	$A_S^{IV} - A_S^{(.)}$	$A_S^{IV}$	$A_S^{IV} - A_S^{(\%)}$	
0.9	-4.4	0.9	0	0.91	+1	0.87	-3	0.89	-1			
0.8	-6.25	0.8	0	0.79	-1	0.76	-4	0.77	-3			
0.7	-7.0	0.74	+4	0.72	+2	0.7	0	0.7	0			
0.6	-8.1	0.64	+4	0.6	0	0.6	0	0.59	-1			
0.5	-8.9	0.55	+5	0.5	0	0.52	+2	0.51	+1			
0.4	-10.0	0.43	+3	0.36	-4	0.41	+1	0.38	-2			
0.3	-11.0	0.33	+3	0.26	-4	0.32	+2	0.28	-2			
0.2	-12.5	0.2	0	0.14	-6	0.21	+1	0.17	-3			
0.1	-14.7	0.09	-1	~		~						

Let

$$x_0^{iv} = \frac{(x_0'' + x_0''')}{2} = 2.227$$

$$k^{iv} = \frac{(k'' + k''')}{2} = 0.018$$

Then

$$A_{s1} = \frac{1}{1 + 0.018 e^{-x/2.227}}$$

The results shown in column 10 in Table I are very good, the error being very small over a large part of the range.  $A_s^{iv}$  is also plotted in Fig. 12 to compare with the other two curves.

At this point, we may find, from the above example, that an accurate determination of  $(k, x_0)$  needs more than just the simple procedure based on two known points. Put in an algorithm form the procedure should be:

- 1) Choose at least three known points in the intermediate range of  $A_s$ , e.g. 0.5 ~ 0.7).
- 2) For each two points in the total set, use Eqs. 4 and 5 to determine the corresponding  $(x_0, k)$  value.
- 3) Choose an appropriate average value of  $(x_0, k)$  to obtain the best result.

Another example is now given. We will test our formula for this case.

#### Example 2

Interference: white noise (PB 1000 words test method is used).  
BW:  $\geq 6$  kHz.

The actual curve for such a case is seen on p. 2-5 of Ref. 44, which is plotted as example (2) on Fig. 6 and the solid curve on Fig. 13.

Step 1. Choose  $(A_s, x)$  pair.

We choose three such pairs:

$$(A_{s1}, x_1) = (0.7, 6)$$

$$(A_{s2}, x_2) = (0.6, 2.5)$$

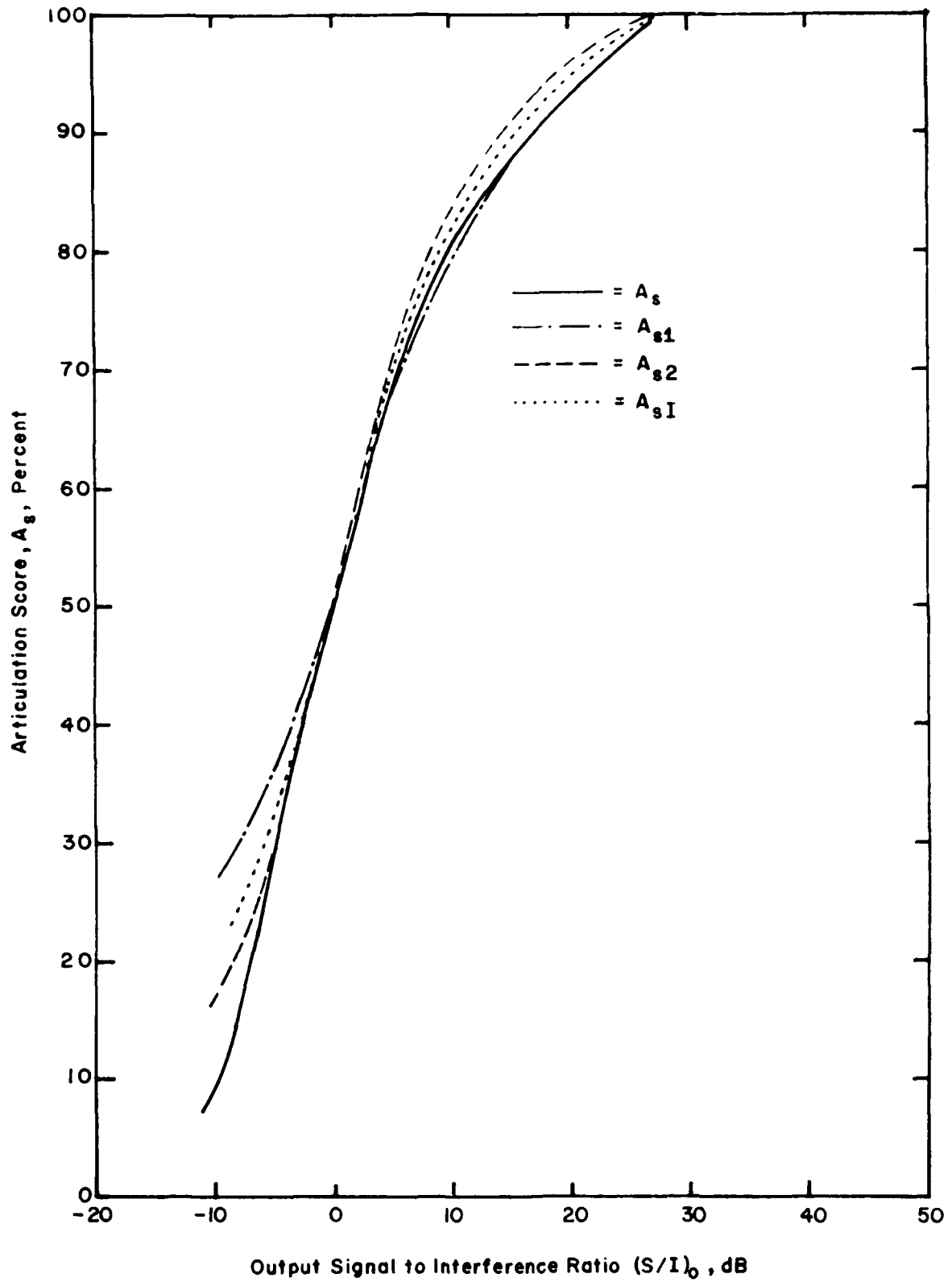


Figure 13

Comparison of Experimental and Modeled  
Degradation Curves: Analog Case, Example 2

$$(A_{s3}, x_3) = (0.5, 0)$$

Step 2. Calculate  $(x_{oi}, k_i)$   $i = 1, 2, \dots$

$$(x_{o1}, k_1) = (7.92, 0.914) \text{ based on } (A_{s1}, x_1)(A_{s2}, x_2)$$

$$(x_{o2}, k_2) = (6.166, 1) \text{ based on } (A_{s2}, x_2)(A_{s3}, x_3)$$

Step 3. Choose the average value.

$$(x_{oI}, k_I) = (7.043, 0.957)$$

$A'_{s1}$ ,  $A'_{s2}$  and  $A_{sI}$  are calculated using the corresponding values  $(x_{o1}, k_1)$ ,  $(x_{o2}, k_2)$  and  $(x_{oI}, k_I)$ . Table II shows the results.

TABLE II  
COMPARISON OF APPROXIMATION FORMULA FOR ARTICULATION SCORE ( $A_s$ )  
WITH EXPERIMENTAL CURVE (EXAMPLE 2)

$A_s$	$x(\text{dB})$	$A'_{s1}$	$A'_{s2}$	$A_{sI}$	$A'_{s1} - A_s$	$A'_{s2} - A_s$	$A_{sI} - A_s$
90	17	90	94	92	0	+ 4	+ 2
80	10	79	83.5	81	- 1	+ 3.5	+ 1
70	6	70	72.6	71	0	+ 2.6	+ 1
60	2.5	60	60	60	0	0	0
50	0	52	50	51	+ 2	0	+ 1
40	-3	43	38	40.5	+ 3	- 2	+ 0.5
30	-5	37	31	34	+ 7	+ 1	+ 4.0
20	-7	31	24	27.5	+ 11	+ 4	+ 7.5
10	-9.5	24.5	18	21.0	+ 14.5	+ 8	+ 11

$A_{S1}$ ,  $A_{S2}$  and  $A_{SI}$  are plotted in Fig. 13 for comparison. It is easily seen in Table II that  $A_{SI}$  is an improvement over  $A_{S1}$  and  $A_{S2}$ , although  $A_{S1}$  and  $A_{S2}$  both show superiority in certain regions.

An interesting thing in this case is the positive error occurring in all three approximations for the low  $A_S$  value range. For the high  $A_S$  range, however, the proper choice of  $(x_0, k)$  results in a very small error.

In order to improve the fit of the curve, it may be practical to make use of a modification factor, MF, in Eq. 1, thus

$$A_S = \frac{1}{1 + k e^{-x/(x_0 MF)}} \quad |x| \gg | \quad (6)$$

where MF is used to more accurately fit the real curve in specific regions of a given curve.

One way of choosing the value of the MF can be done in this way:

When  $A_S = 0.2 \quad x = -7$

$A_S = 0.1 \quad x = -9.5$

Then, based on these two values, using  $A_S = \frac{1}{1 + 0.957 e^{-x_i/x_0}}$

for (0.2, -7), with  $k = 0.957$ .

$$x_0'' = x_i / \ln \left( \frac{1 - A_{Si}}{0.957 A_i} \right)$$

$$= 4.87$$

For (0.1, -9.5), with  $k = 0.957$

$$x_0'' = 4.24$$

Comparing  $x_0''$  of 4.87 or 4.27 with the  $x_{0I} = 7.043$ , we find that, for low  $(S/I)_0$ ,  $x_0$  is significantly reduced. Then MF may be defined as

$$MF = \frac{(4.87 + 4.24)}{2 \times 7.043}$$

$$= 0.647$$

Then, a complete description of the performance curve for this interference is

$$A_s = \frac{1}{1 + 0.957 e^{-x/7.043}} \quad \text{for } A_0 = 0.5$$

$$= \frac{1}{1 + 0.957 e^{-x/7.043} MF} \quad MF = 0.647 \quad \text{for } A_0 = 0.5$$

Another example will be given in the following, where interference is a low-frequency single-tone (sine wave) very different from the noise and pulsed-type interference mentioned in examples 1 and 2.

### Example 3

Interference 250 Hz, CW interference.

The  $A_s$  vs  $(S/I)_0$  curve is seen on p. 3-10 (Ref. 44), plotted as a solid line in Fig. 14<sup>0</sup> (9) on Fig. 6).

$$\text{Let } (A_{s1}, x_1) = (0.7, -35 \text{ dB})$$

$$(A_{s2}, x_2) = (0.6, -37 \text{ dB})$$

$$(A_{s3}, x_3) = (0.5, -39 \text{ dB})$$

Then

$$(x'_0, k') = (4.53, 0.000189) \text{ based on } (A_{s1}, x_1)(A_{s2}, x_2)$$

$$(x''_0, k'') = (4.93, 0.000367) \text{ based on } (A_{s2}, x_2)(A_{s3}, x_3)$$

$$(x_{oI}, k_{oI}) = (4.73, 0.000298)$$

$$x_{oI} = \frac{x'_0 + x''_0}{2}, \quad k_{oI} = \frac{k' + k''}{2}$$

The results for these values are shown in Table III.

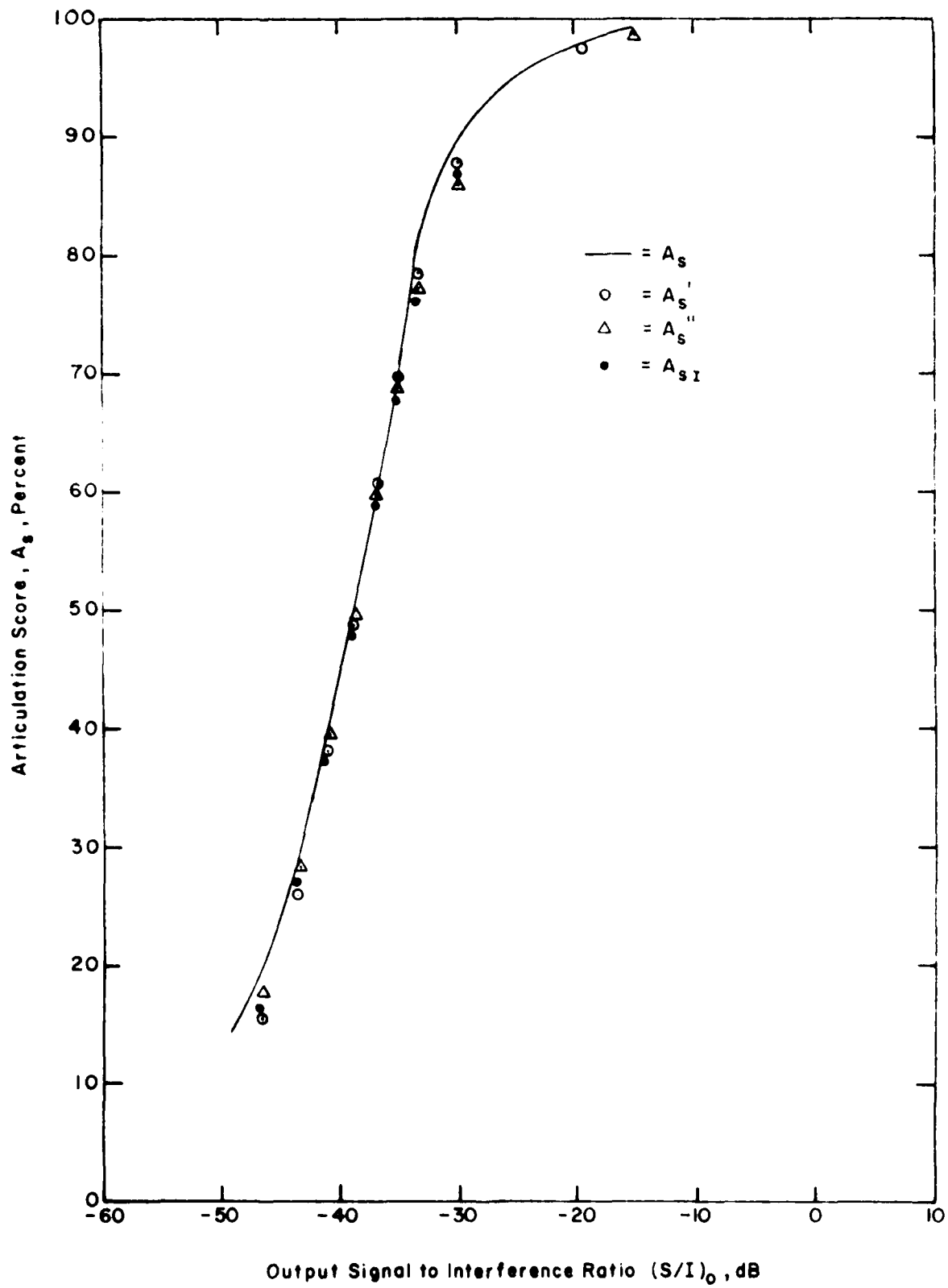


Figure 14

Comparison of Experimental and Modeled  
Degradation Curves; Analog Case, Example 3

TABLE III

COMPARISON OF APPROXIMATION FORMULA FOR ARTICULATION SCORE ( $A_s$ )  
WITH EXPERIMENTAL CURVE (EXAMPLE 3)

$A_s$	x (dB)	$A'_s$	$A''_s$	$A_{sI}$	$A'_s - A_s$ (%)	$A''_s - A_s$ (%)	$A_{sI} - A_s$ (%)
1.0	-15	0.995	0.994	1.0	-0.5	-0.6	0
0.9	-30	0.876	0.86	0.864	-2.4	-4	-3.6
0.8	-33	0.784	0.77	0.77	-1.6	-3	-3.0
0.7	-38	0.70	0.69	0.687	0	-1	-1.3
0.6	-37	0.60	0.60	0.59	0	0	-1
0.5	-39	0.49	0.50	0.49	-1	0	-1
0.4	-41	0.38	0.40	0.38	-2	0	-2
0.3	-43.5	0.26	0.236	0.27	-4	-1.4	-3
0.2	-46.5	0.156	0.18	0.162	-4.4	-2.0	-3.8

It is interesting to see that, in this case,  $A'_s$ ,  $A''_s$  and  $A_{sI}$  are almost equally good approximations, with  $A'_s$  showing a slight overall superiority. The reason for such an occurrence can be seen in the following comparison.

a) In example 1:

$$\frac{x_0'' - x_0'}{x_0'' + x_0'} = \frac{0.57}{2.2} = 0.26$$

b) In example 2:

$$\frac{x_{01} - x_{02}}{x_{01} + x_{02}} = \frac{1.75}{7.04} = 0.25$$

c) In example 3:

$$\frac{\frac{x_0^1 - x_0^2}{x_0^1 + x_0^2} - \frac{0.4}{4.73}}{2} = 0.085$$

For this case,  $A_S''$  is chosen as the desired expression, i.e.

$$A_S = \frac{1}{1 + 0.000367 e^{-x/493}}$$

for single tone 250 Hz interference.

Another interesting thing that is worth noting in this example is the overall pessimistic prediction for three expressions in both high and low  $(S/I)_0$  regions. This contrasts significantly with what we have seen in example 2, where an overall "optimistic" prediction in the mentioned regions is indicated. This tells us that, for this interference, the performance for the high  $(S/I)_0$  region improves much more quickly than is predicted in the medium  $A_S$  region. In the low  $(S/I)_0$  range, the degradation follows the predicted trend without too much deviation.

In example 2, however, the situation is quite the converse. In the high  $(S/I)_0$  region, the predicted performance matches the actual value quite accurately. In the low  $(S/I)_0$  region, however, the degradation increases more quickly than predicted.

### 3.2 Digital Systems

Whereas in analog systems a common measure of performance is articulation score, in digital systems probability of error is usually adopted. This may be expressed in terms of individual bits, symbols or words, as is appropriate in individual cases. The error probability measure is, thus, a negative measure when compared to that used in analog systems, i.e. the lower the error probability, the better is the system performance.

Typical results for bit-error probability for digital systems are shown in Fig. 17 for interference due to random noise and sine (continuous) waves, where the ordinate is bit-error rate  $P_e$ , and the abscissa is the predetection signal-to-interference (or noise) ratio in dB.

For some types of interference, as shown on Fig. 18, the derived functional relations of  $P_e$  with respect to  $(S/I)_0$  for various detection processes have been defined in terms of simple analytic functions. For other cases, such as the CPFSK system, this is not the case. Indeed, the

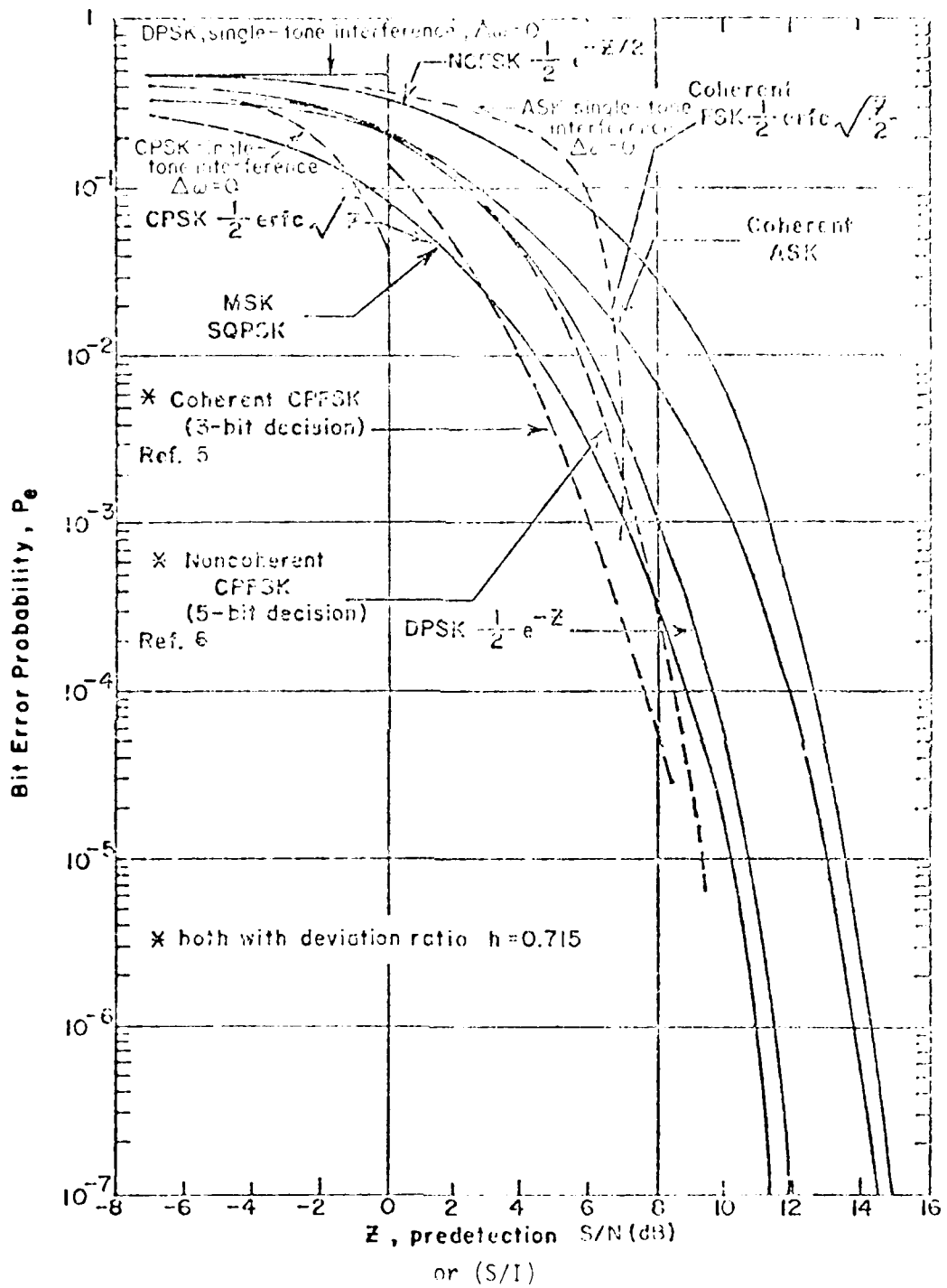


Figure 15 Error Probability for Various Digital Systems. Effects of CW Interference

functional form is very complicated. Nevertheless, as in the analog case, we seek expressions that can give us a reasonable fit within certain desired ranges.

To begin with, we characterize the trend of probability of error for binary system curves as follows:

- a) When  $(S/I)$  approaches  $\infty$ ,  $P_e$  approaches 0; while, when  $(S/I)$  approaches 0, 0.5 serves as the upper limit.
- b)  $P_e$  usually varies with  $(S/I)$  in exponential form.
- c) Generally speaking, for  $S/I = 1$  (or 0 dB),  $P_e$  values are not acceptable in most systems. The region of  $P_e$  that one is most interested in ranges from  $10^{-2}$  to better than  $10^{-6}$ , i.e.  $S/N$  well above 0 dB.

Because of the general shape of the curves on Fig. 15, the validity of the following relationships is examined:

$$P_e = \frac{1}{2} \exp(-x^n/x_0) \quad (7)$$

where  $n$  and  $x_0$  are two parameters whose values can be selected to match the performances of different systems in the presence of different types of interference.

$x$  is the predetection signal-to-interference ratio, expressed in the ordinary ratio. Therefore, it varies from 0 to  $\infty$  (in dB, from  $-\infty$  to  $+\infty$ ).

From Eq. 7, we find that  $P_e$  approaches 0 as  $x$  goes to  $\infty$ , while it goes to 1/2 as  $x$  approaches 0, which satisfies condition (a) above.

To determine  $n$  and  $x_0$ , we need at least two known points  $(x_i, P_{ei})$   $i = 1, 2$ . Then,  $n$  and  $x_0$  can be determined from

$$n = \frac{\ln \frac{(1 - 2P_{e1})}{(1 - 2P_{e2})}}{\ln \frac{x_1}{x_2}} \quad (8)$$

$$x_0 = \frac{x_1^n}{\ln \frac{1}{1 - 2P_{e1}}} \quad (9)$$

Since this is an approximation, good accuracy will be obtained only in certain regions, beyond which the deviation may become large, or additional correction must be added.

To see how well Eq. 7 meets requirements, two examples are given in the following:

Example 1

DPSK system with random (Gaussian) noise interference. In this case, as shown on Fig. 15, the functional dependence is:

$$P_e = \frac{1}{2} e^{-z}$$

Since this is of the same form as Eq. 7, the values of  $r = 1$  and  $x_0 = 1$  can be established by inspection. Thus, the exact expression is obtained for all values of  $x$ .

Example 2

Coherent PSK system interfered by random Gaussian noise.

Two sets of known points are picked to determine  $(n, x_0)$  respectively.

For the first set

$$x_1 = 5 \text{ dB (3.162)}, P_{e1} = 0.0064$$

$$x_2 = 7 \text{ dB (5.01)}, P_{e2} = 7.6 \times 10^{-4}$$

From Eqs. 8 and 9

$$n_1 = 0.865$$

$$x_{01} = 0.621$$

For the second set

$$x_1 = 7 \text{ dB (5.01)}, P_{e1} = 7.6 \times 10^{-4}$$

$$x_2 = 9 \text{ dB (7.94)}, P_{e2} = 3.3 \times 10^{-5}$$

and

$$n_2 = 0.856$$

$$x_{02} = 0.612$$

The two sets of values ( $x_0$ ,  $n$ ) are quite close, and we choose the intermediate value as

$$x_0 = 0.618$$

$$n = 0.86$$

Figure 16 and Table IV compare the original and approximated data.

TABLE IV  
COMPARISON OF COHERENT PSK THEORETICAL PERFORMANCE CURVE IN GAUSSIAN NOISE WITH APPROXIMATED CURVE

$x(\text{dB})$	$x(\text{numerical})$	$P_e(\text{exact})$	$P_e = \frac{1}{2} e^{-\frac{x}{0.618} \cdot 0.86}$
- 5	0.316	$2.13 \times 10^{-1}$	$2.7 \times 10^{-1}$
0	1	$7.9 \times 10^{-2}$	$9.9 \times 10^{-2}$
3	1.995	$2.3 \times 10^{-2}$	$2.67 \times 10^{-2}$
5	3.16	$6.0 \times 10^{-3}$	$6.4 \times 10^{-3}$
7	5.01	$6.5 \times 10^{-4}$	$7.7 \times 10^{-4}$
9	7.94	$3.3 \times 10^{-5}$	$3.3 \times 10^{-5}$
10	10.0	$5.0 \times 10^{-6}$	$4.1 \times 10^{-6}$
15	31.62	$\sim$	$1.0 \times 10^{-14}$

We find from Table IV that good accuracy is obtained from  $P_e = 10^{-2}$  down to  $P_e = 10^{-6}$ . It should be noted that the exact form of  $P_e$  for CPSK is  $\frac{1}{2} \text{erfc}(\sqrt{x})$ .

Let us now examine the parameters  $n$  and  $x_0$  of Eq. 7. First observe that for

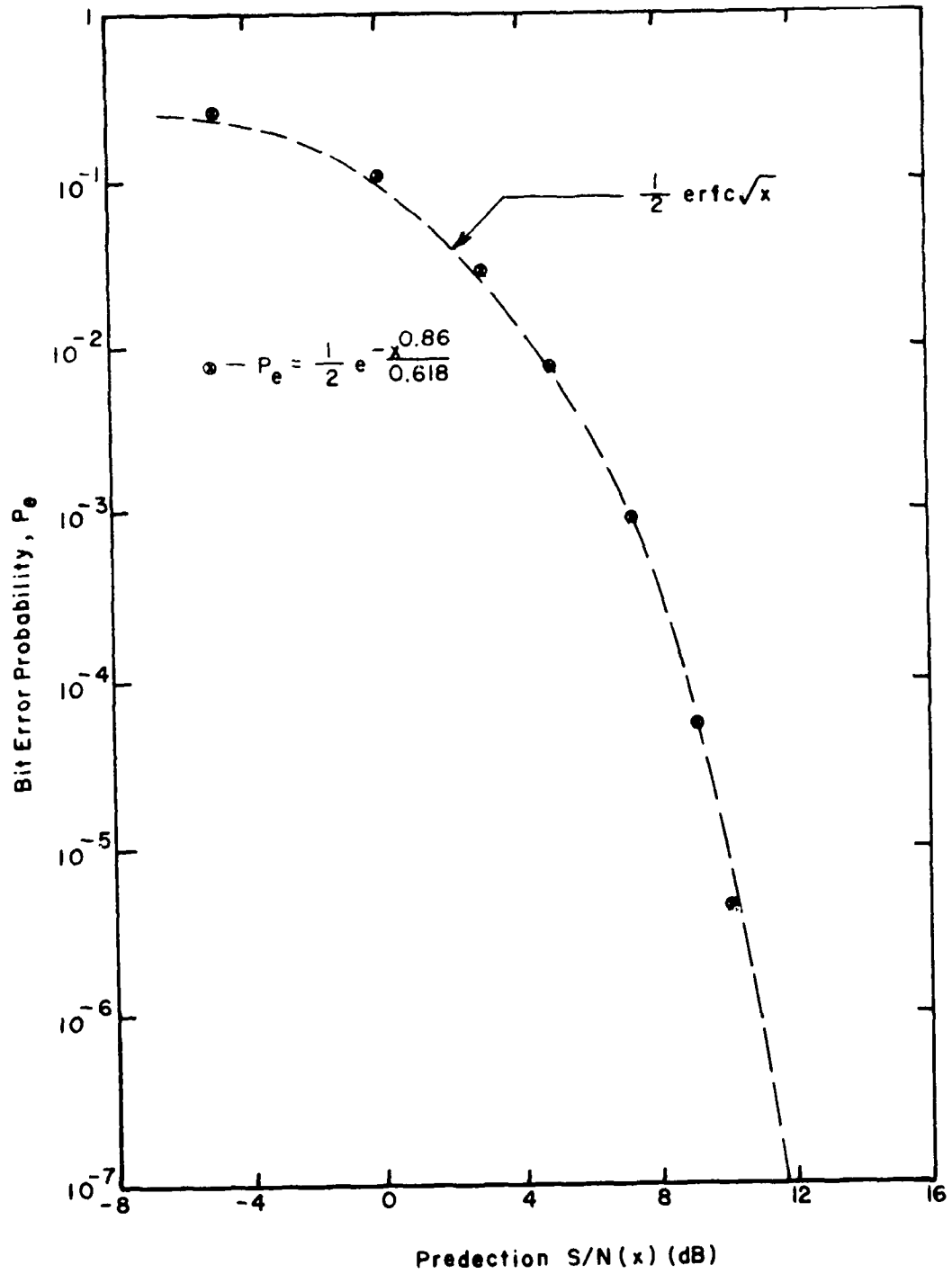


Figure 16 Comparison of Modeled and Theoretical Error Probability Curves: Digital Case, Example 2

$$x = 1 (S = N \text{ or } \frac{S}{N} = 0 \text{ dB})$$

$$P_e = \frac{1}{2} e^{-\frac{1}{x_0}} \quad (10)$$

or 
$$x_0 = \frac{-1}{\ln 2P_e} \text{ independent of } n \quad (11)$$

Now select  $x_0$  such that  $P_e$  for  $x = 1$  takes the value  $10^{-3}$  (any other value could be selected, however  $10^{-3}$  is perhaps a mean value of  $P_e$  of interest). We find that  $x_0 = 0.161$ . Figure 17 shows plots of Eq. 7 for this value of  $x_0$  for various values of  $n$ . Note that  $n$  determines the shape of the curve and that the value of  $n = \infty$  matches the theoretical curve for CW interference.

Secondly, observe that the curves on Fig. 15 are of the same general shape except that they are shifted along the horizontal axis. In other words, a transformation (on the dB scale) of the form

$$x'(\text{dB}) = x(\text{dB}) + x_s(\text{dB}) \quad (12)$$

applies. Or, numerically,

$$x' = x x_s$$

Using (7), we have

$$P_e = \frac{1}{2} e^{-\left(\frac{x'}{x_s}\right)^n \frac{1}{x_0}} \quad (13)$$

as a more general form, where  $x'$  is the actual value of  $S/N$  and  $x_s$  is the numerical value of  $x'$  at which the reference value of  $P_e$ ,  $P_{e0}$ , is obtained, and which defines  $x_0$ , i.e. from Eq. 11,

$$x_0 = \frac{1}{-(\ln 2P_{e0})}$$

If  $x_s$  is expressed in dB,  $x_s$  as given in (13) is

$$x_s = e^{0.23 x_s(\text{dB})}$$

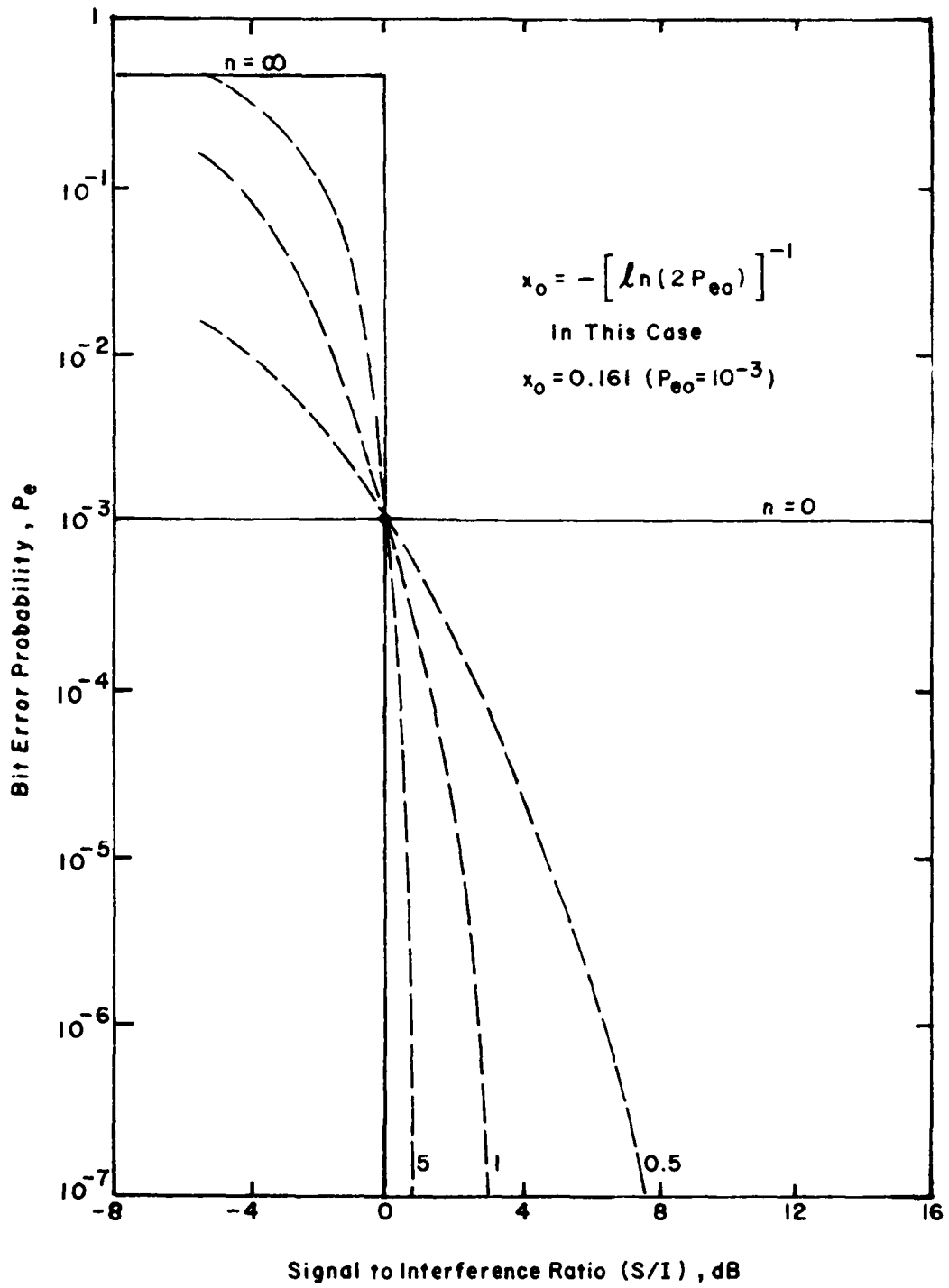


Figure 17 The Function  $P_e = \frac{1}{2} e^{-x^n/x_0}$

Finally, note that Eq. 7 can be written in the original form if we let  $x = x'$  and  $x_0$  is replaced with  $x_{00}$ :

$$x_{00} = x_s^n x_0$$

Based on the above discussion, to obtain the parameter values in Eq. 7 graphically, proceed as follows:

Step I

Prepare the reference curve as in Fig. 17, where Eq. 7 is plotted against  $x$ , with  $n$  as the parameter and all the curves pass the point  $x = 1(0 \text{ dB})$ ,  $P_{e0}$ .  $P_{e0}$  should be chosen as the one that lies well within the desired ranges of  $P_e$  of interest. In Fig. 17  $P_{e0} = 10^{-3}$ . Note that the abscissa for  $x$  is given in dB values instead of the ordinary ratio. Calculate  $x_0$  using

$$x_0 = - \left[ \ln(2P_{e0}) \right]^{-1} \quad (14)$$

instead of Eq. 11.

Step II

Compare the actual curve to be described; record the value of  $x (= x_s)$  corresponding to  $P_{e0}$ .

Step III

Shift the curve to the new position where it passes through  $P_{e0}$  at  $x = 1(0 \text{ dB})$ .

Step IV

Find the value of  $n$  that best fits the real curve in the desired range.

Step V

With  $n$  determined, compute

$$x_{00} = x_0 \left[ \exp(0.23)(x_s) \right]^n \quad (15)$$

where  $x_s$  and  $n$  are the results of Steps II and IV, respectively.

We then have

$$P_e = \frac{1}{2} e^{-\frac{x_s^n}{x_0^n}} \quad (16)$$

which is similar to (7) but in which  $x_s$  is explicitly defined.

Thus, one can explore the possibility of expressing any combination of signal and interference performance in terms of the parameters  $n$ ,  $x_0$ , and  $x_s$ .

#### 4.0 CONCLUSIONS

In this report information has been collected showing the relationships between signal-to-interference ratio and the degradation to be experienced in typical digital and analog systems, and it has been shown that analytical relations can be postulated that closely match actual (empirical) data.

There are two basic tasks to be completed. The first is to demonstrate how the models developed can be effectively implemented in interference prediction work. This will include an evaluation of the accuracies obtainable with various important combinations of signal modulation and interference, and the refinement of the model where necessary.

The second task is to try to generalize the concepts so as to permit making estimates of degradation without reference to intermediate empirical results. The objective here is to differentiate types of signal modulation and interference by assigning values to a minimum number of parameters, and to make predictions entirely on the basis of these parameters.

## 5.0 REFERENCES

1. H. Taub and Donald L. Schilling, PRINCIPLES OF COMMUNICATIONS SYSTEMS, McGraw-Hill, 1971.
2. M. D. Srinath and P. K. Rajasekaran, AN INTRODUCTION TO STATISTICAL SIGNAL PROCESSING WITH APPLICATION, John Wiley and Sons, 1979.
3. S. Stein and J. J. Jones, MODERN COMMUNICATION PRINCIPLES, McGraw-Hill, New York, 1967.
4. W. David Gregg, ANALOG AND DIGITAL COMMUNICATIONS, John Wiley and Sons, New York, 1977.
5. Thomas A. Schonhoff, "Symbol error probabilities for M-ary CPFSK: coherent and noncoherent detection," IEEE TRANS COMMUNICATIONS, vol COM-24, pp 644-652, June 1976.
6. William P. Osborne and Michael B. Luntz, "Coherent and noncoherent detection of CPFSK," IEEE TRANS COMMUNICATIONS, vol COM-22, pp 1023-1036, Aug 74.
7. Steven A. Gronemeyer and Alan L. Mcbridge, "MSK and offset QPSK modulation," IEEE TRANS COMMUNICATIONS, vol COM-24, pp 809-820, Aug 76.
8. Rudi de Buda, "Coherent demodulation of frequency-shift keying with low deviation ratio," IEEE TRANS COMMUNICATION TECH, vol COM-20, pp 429-435, June 72.
9. H. Robert Mathwich, Joseph F. Balcewicz and Martin Hecht, "The effect of tandem band and amplitude limiting on the  $E_b/V_o$  performance of minimum (frequency) shift keying (MSK)," IEEE TRANS COMMUNICATIONS, vol COM-22, pp 1525-1540, Oct 74.
10. John D. Oetting, "A comparison of modulation techniques for digital radio," IEEE TRANS COMMUNICATIONS, vol COM-27, pp 1752-1756, Dec 79.
11. Louis S. Metzger, "Performance of phase comparison sinusoidal frequency shift keying," IEEE TRANS COMMUNICATIONS, vol COM-26, pp 1250-1253, Aug 78.
12. ENGINEERING DESIGN HANDBOOK: ELECTROMAGNETIC COMPATIBILITY, DARCOM-P706-410, AD A038803, Mar 77, Ch 3.
13. COMMUNICATIONS/ELECTRONICS RECEIVER PERFORMANCE DEGRADATION HANDBOOK, (2nd edition), ESD-TR-75-013, Aug 75.
14. Frank G. Splitt, "Comparative performance of digital data transmission systems in the presence of CW interference," IEEE TRANS COMMUN SYST, vol. CS-10, pp 169-177, June 62.

15. A. S. Rosenbaum, "PSK error performance with Gaussian noise and interference," BELL SYST TECH J, vol 48, pp 413-443, Feb 69.
16. M. J. Massaro, "Error performance of M-ary noncoherent FSK in the presence of CW tone interference," IEEE TRANS COMM, vol COM-23, pp 1367-1369, Nov 75.
17. J. J. Jones, "FSK and DPSK performance in a mixture of CW tone and random noise interference," IEEE TRANS COMMUN TECHNOL, vol COM-18, pp 693-695, Oct 70.
18. R. E. Ziemer, "Error probabilities due to additive combinations of Gaussian and impulsive noise," IEEE TRANS COMMUN TECHNOL, vol COM-15, pp 471-474, June 67.
19. W. J. Richter and T. I. Smits, "Signal design and error rate of an impulsive noise channel," IEEE TRANS COMMUN TECHNOL, vol COM-19, pp 446-458, Aug 71.
20. D. Middleton, "Statistical-physical models of man-made radio noise. Part I: First-order probability models of the instantaneous amplitude," Office of Telecommunications, OT Report 74-36, Apr 74, (U.S. Government Printing Office, Wash., DC 20402).
21. D. Middleton, "Statistical-physical models of man-made and natural radio noise. Part II: First-order probability models of the envelope and phase," Office of Telecommunications, OT Report 76-86, Apr 76 (National Technical Information Service, Springfield, VA.).
22. R. A. Wainwright, "On the potential advantage of a smearing-desmearing filter technique in overcoming impulse noise problems in data systems," IEEE TRANS COMM SYST, vol. CS-9, pp. 362-366, Dec. 61.
23. A. A. Giordano and H. E. Nichols, "Simulated error rate performance of nonlinear receivers in atmospheric noise," PROC. NATIONAL TELECOMMUNICATIONS CONF., pp. 20.2/1-4.
24. M. E. Mitchell, "Performance of error-correcting codes," IEEE TRANS COMMUN SYSTEMS, vol. CS-10, pp 72-85, March 62.
25. G. C. Clark, Jr. and R. C. Davis, "Two recent applications of error-correcting coding to communication systems design," IEEE TRANS COMMUN TECHNOL, vol. COM-19, pp. 856-863, Oct. 71.
26. A. Brind'amour and K. Feher, "Design and evaluation of a convolutional codec in additive white Gaussian noise, sinusoidal interference and intersymbol interference environment," IEEE TRANS COMMUN, vol. COM-28, pp 391-395, Mar. 80.
27. P. D. Newhouse, "Bounds on the spectrum of a CHIRP pulse," IEEE TRANS EMC, vol. EMC-15, no. 1, pp 27-33, Feb 73.

28. H. L. Van Trees, DETECTION, ESTIMATION AND MODULATION THEORY, John Wiley and Sons, 1971, Parts II and III.
29. J. V. Difrancio and W. L. Rubin, RADAR DETECTION, Prentice-Hall, 1968, Part IV.
30. M. I. Skolnik, INTRODUCTION TO RADAR, McGraw-Hill, New York, 1980.
31. F. E. Nathanson, RADAR DESIGN PRINCIPLES, McGraw-Hill, New York, 1969, Ch. 9.
32. W. M. Hall and H. R. Ward, "Signal to noise loss in moving target indicator," PROC. IEEE, vol. 56, pp 233-234, Feb. 68.
33. N. Lichtenstein, "The susceptibility of MTI system to white noise," IEEE TRANS. AEROSPACE & ELECTRONIC SYSTEMS, vol. AES-11, pp 781-784, Sep. 75.
34. A. W. Rihaczek, PRINCIPLES OF HIGH RESOLUTION RADAR, McGraw-Hill, New York, 1969, Ch. 10.
35. F. E. Nathanson and J. P. Reilly, "Clutter statistics which affect radar performance analysis," AEROSPACE AND ELECTRONIC SYSTEMS TECHNICAL CONVENTION RECORD, 1967, pp. 386-398.
36. D. K. Barton, RADARS, Vol. V-Radar clutter, Artech House, 1977.
37. D. C. Scheler, "Detection performance of logarithmic receivers employing video integrators," IEEE TRANS AEROSPACE AND ELECTRONIC SYSTEMS, vol. AES-15, pp. 831-839, Nov. 79.
38. Leon Camp, UNDERWATER ACOUSTICS, Wiley-Interscience, 1970, Ch. 9 and 10.
39. J. J. Nicholas, Jr., "Cochannel interference analysis between spaceborne and terrestrial radars," IEEE TRANS AEROSPACE AND ELECTRONIC SYSTEMS, vol. AES-14, pp. 803-812, Sep. 78.
40. M. N. Lustgarten and R.D. Grigg, "Effects of radar interference on search radar performance," RECORD OF 1977 IEEE INTERNATIONAL SYMPOSIUM ON EMC, Aug 1977, pp 190-195.
41. R. C. Pierstorff, P. Rosenthal, and C. M. Hanes, "Simulation of radar/radar interference at RF for the evaluation of interference effects on operator performance," RECORD OF 1977 IEEE INTERNATIONAL SYMPOSIUM ON EMC, Aug 1977, pp 196-200.
42. Louis Maisel, "Sidelobe blanking systems," IEEE TRANS AEROSPACE AND ELECTRONIC SYSTEMS, vol. AES-4, pp 174-180, Mar 68.



END

DATE  
FILMED

5 8 1

DTIC